International Journal of Non–Linear Mechanics 169 (2025) 104936

Contents lists available at ScienceDirect

International Journal of Non-Linear Mechanics

journal homepage: www.elsevier.com/locate/nlm

# Surface instability of a finitely deformed magnetoelastic half-space

Davood Shahsavari, Prashant Saxena *

*Glasgow Computational Engineering Centre, James Watt School of Engineering University of Glasgow, Glasgow G12 8LT, UK*

ARTICLE INFO

*Keywords:*
Surface instability
Magnetoelasticity
Wrinkling
Incremental theory

ABSTRACT

Magnetorheological elastomers (MREs) are soft solids that can undergo large and reversible deformation in the presence of an externally applied magnetic field. This coupled magneto-mechanical response can be used for active control of surface roughness and actuation in engineering applications by exploiting the reversible instabilities in these materials. In this work, we develop a general mathematical formulation to analyse the surface instabilities of a finitely deformed and magnetised MRE half-space and find the critical stretch that causes bifurcation of the solution of the resulting partial differential equations. The equations are derived using a variational approach in the reference configuration and the null-space relating the incremental solutions is presented to provide a basis for post-bifurcation analysis. Details of the numerical calculations are presented to clearly identify and discount non-physical solutions. Stability phase diagrams are presented to analyse the effect of material parameters and strength/direction of magnetic field.

## 1. Introduction

Soft solids undergoing surface undulations due to compressive stresses is a well documented phenomenon [1,2]. In elastic solids, these reversible wrinkles, creases, or folds are often modelled as a form of surface instability [3–8]. Although the mathematical modelling of wrinkles for hyperelastic solids with a first order stability analysis is well understood, a general framework to model surface instabilities in a multi-physics scenario is lacking. In this work, we present a variational approach to analyse the surface instabilities of a finitely deformed and magnetised magnetoelastic half-space. In particular, we clarify issues around non-physical numerical solutions that are undocumented in literature and present new numerical results for magnetic field applied parallel and perpendicular to the surface.

Magnetorheological elastomers (MREs) are a class of smart materials that consist of magnetisable particles, ranging in size from micron to nanoscale, dispersed within a polymer matrix. The observed characteristics of this material indicate a propensity to show a mechanical reaction to external magnetic fields. Magnetoelastic effects can be categorised into two distinct groups, namely direct effects and indirect effects [9]. The direct magnetoelastic effects are most well-recognised in the literature and are concerned with changes in dimensions and stiffness due to an external magnetic field. Indirect effects pertain to alterations in a material's magnetic susceptibility resulting from mechanical stress [9,10]. James Joule [11] first identified magnetostriction in 1842 during his investigation of an iron sample. Over the last several decades, much research has focused on investigating and simulating the mechanics of MREs by focussing on the magnetoelastic effects [12]. Multiple researchers have investigated experimental techniques to quantify the mechanical response of MREs in the presence of an external magnetic field [1,13–15].

The modelling of MREs involves several methods, such as macro-continuum-based models, micro-particle interaction-based models, and data-driven phenomenological models [16]. Continuum models incorporate nonlinear coupling between magnetic and mechanical fields, thereby enabling the analysis of the magneto-mechanical behaviour of MREs under complex loading and boundary conditions [17,18]. Dorfmann and Ogden [18] introduced constitutive formulations based on modified free energy functions and the total stress tensor to develop fully coupled nonlinear field theories. It has been shown that either one of the magnetic induction, magnetic field or magnetisation vectors can act as an independent variable in the formulation [19–22]. Bustamante et al. [23] derived the universal relations for nonlinear magnetoelastostatics; this was further expanded by Kumar et al. [24] for coupled electro-magneto-elastic soft materials.

Biot formulated the bifurcation theory [3,25] to describe surface instability of an incompressible neo-Hookean elastic half-space by taking into account the existence of wavelike/smooth undulation modes on the surface. Numerous elastic systems, both biological and synthetic, exhibit Biot-like surface instability under large deformation. This instability may contribute to various aspects of morphogenesis in biological systems

* Corresponding author.
*E-mail address:* prashant.saxena@glasgow.ac.uk (P. Saxena).

https://doi.org/10.1016/j.ijnonlinmec.2024.104936
Received 13 September 2024; Accepted 24 October 2024
Available online 19 November 2024

including development of fingerprints [26], retina folds [27], the placental villous tree [28], and the sulci of the brain cortex [29]. It has also been associated with plastic surface instabilities in industrial applications [30].

A considerable amount of theoretical [3,6,31–33], computational [34,35], and experimental [30,36] investigations have been conducted due to the wide range of possible applications of surface instability phenomena in soft materials. The aforementioned publications explored a diverse range of surface instabilities, including wrinkling, cavitation, creasing, ridging, folding, and fringe.

Surface instability of electro-elastic [37] and magneto-elastic [38,39] elastomers has been extensively studied both theoretically and experimentally over the past two decades because of their applications in micro/nano-electromechanical systems (MEMS/NEMS), magnetostrictive actuation, soft robotics, pattern formation and morphology control, energy harvesting and sensing, soft electronics, biomedical and wearable devices [40–44]. Otténio et al. [5] used the incremental theory [45] to analyse the surface instability of a magnetoelastic half-space that is subjected to perpendicular magnetic field with low and moderate magnitudes. The same incremental formulation was used by Saxena and Ogden [46,47] to study the dynamic problem of wave propagation. Rudykh and Bertoldi [48] studied this surface instability for a periodically layered MRE composite using a micromechanics based formulation. Dorfmann et al. [49] utilised an equivalent framework to analyse surface instability in an electroelastic neo-Hookean half-space. Danas et al. [1] showed experimentally that surface instability of a pre-stretched MRE block can be modulated by a perpendicular magnetic field. In this paper, we develop a general formulation to analyse the surface instabilities of a finitely deformed half-space under both perpendicular and parallel magnetic fields. A variational approach is used to clearly identify all the relevant partial differential equations and the solution variables [22]. Solution of the bifurcation equations requires derivation of the null-space of the matrix system of equations that sets a foundation for post-bifurcation analysis [6]. A numerical method is implemented using Maple and Mathematica programming environments to track all the potential solutions of this highly nonlinear problem, identify the system's limit points, and discard non-physical solutions.

### 1.1. Notation

Scalar variables are presented in normal weight font, while first or second-order tensors are denoted with bold weight font. Circular brackets () are used to indicate the parameters of a function while square brackets [ ] are used to group mathematical expressions. A comma in a subscript represents a partial derivative with respect to the in-plane coordinates $(X_1, X_2)$. The scalar product of two vectors $\mathbf{m}$ and $\mathbf{n}$ is denoted by $\mathbf{m}\cdot\mathbf{n}$, and their tensor product is represented by a second-order tensor $\mathbf{A} = \mathbf{m}\otimes\mathbf{n}$. The operation of this second-order tensor $\mathbf{A}$ on a vector $\mathbf{p}$ is given by $\mathbf{A}\cdot\mathbf{p}$. A second-order tensor $\mathbf{A}$ can be expressed in its component form using the matrix notation $A_{ij}$. The scalar product of two tensors $\mathbf{A}$ and $\mathbf{B}$ is defined as $\mathbf{A} : \mathbf{B} = A_{ij}B_{ij}$. The differentiation operator in the reference configuration is denoted as $\nabla_R = \frac{\partial}{\partial \mathbf{X}}$ while the same in the current configuration is denoted as $\nabla = \frac{\partial}{\partial \mathbf{x}}$.

## 2. Nonlinear magnetoelastostatics

Consider an incompressible magnetoelastic solid that occupies a region $\Omega_R$ in its stress-free reference configuration. The deformed configuration is denoted by $\Omega$. The points $\mathbf{X} \in \Omega_R$ and $\mathbf{x} \in \Omega$ are related by a volume-preserving, smooth, and invertible mapping $\chi : \Omega_R \to \Omega$. The deformation gradient is a second order tensor and is denoted as $\mathbf{F} = \nabla_R(\chi)$. The deformation map is smoothly extended to the surrounding free space $\Omega'_R = \mathbb{R}^3 \setminus \Omega_R$, $\chi : \Omega'_R \to \Omega'$ to enable the definition of the referential counterparts of the magnetic variables in vacuum.

The magnetic field $\mathbb{h}$, the magnetic induction $\mathbb{b}$, and the magnetisation $\mathbb{m}$ in $\Omega$ are related as

$$\mathbb{b} = \mu_0\mathbb{h} + \mathbb{m}, \tag{2.1}$$

where $\mu_0$ is the magnetic permeability of the free space. The magnetic field $\mathbb{h}$ and the magnetic induction $\mathbb{b}$ need to satisfy the Maxwell's relations

$$\nabla\times\mathbb{h} = \mathbf{0}, \quad \text{and} \quad \nabla\cdot\mathbb{b} = 0. \tag{2.2}$$

The presence of divergence-free and curl-free conditions motivates the introduction of a magnetic vector potential field $\mathbb{a}$ and a magnetic scalar potential field $\phi$ such that

$$\mathbb{h} = -\nabla\phi, \quad \text{and} \quad \mathbb{b} = \nabla\times\mathbb{a}. \tag{2.3}$$

The corresponding fields in vacuum are denoted by an asterisk and follow the constitutive relation

$$\mathbb{b}^* = \mu_0\mathbb{h}^*. \tag{2.4}$$

Upon defining the referential quantities [19]

$$\mathbb{B} = J\mathbf{F}^{-1}\mathbb{b}, \qquad \mathbb{H} = \mathbf{F}^T\mathbb{h}, \qquad \mathbb{A} = \mathbf{F}^T\mathbb{a}, \qquad \Phi(\mathbf{X}) = \phi(\mathbf{x}(\mathbf{X})) \tag{2.5}$$

Eqs. (2.1)–(2.4) can be reformulated as

$$\nabla_R\times\mathbb{H} = \mathbf{0}, \qquad \nabla_R\cdot\mathbb{B} = 0, \qquad \mathbb{H} = -\nabla_R\Phi, \qquad \mathbb{B} = \nabla_R\times\mathbb{A}, \qquad \mathbb{B}^* = \mu_0 J\mathbf{C}^{-1}\mathbb{H}^*. \tag{2.6}$$

The response of the magnetoelastic solid can be described with the help of a total energy density function denoted by $W(\mathbf{F}, \mathbb{B})$. For an isotropic and incompressible material, it can be shown that the energy is dependent on scalar invariants of the right Cauchy–Green deformation tensor $\mathbf{C}$ and the magnetic induction $\mathbb{B}$

$$I_1 = \mathrm{tr}(\mathbf{C}), \quad I_2 = \frac{1}{2}\left[(\mathrm{tr}\,\mathbf{C})^2 - \left(\mathrm{tr}\,\mathbf{C}^2\right)\right], \quad I_4 = \mathbb{B}\cdot\mathbb{B}, \quad I_5 = \mathbf{C}\mathbb{B}\cdot\mathbb{B}, \quad I_6 = \mathbf{C}\mathbb{B}\cdot\mathbf{C}\mathbb{B}. \tag{2.7}$$

Here we ignore the dependence on the third scalar invariant of $\mathbf{C}$ since the constraint of incompressibility $I_3 = \det(\mathbf{C}) = J^2 = 1$ renders it a constant. The first Piola–Kirchhoff stress $\mathbf{P}$ and the magnetic field $\mathbb{H}$ can be written using the total energy density function as

$$\mathbf{P} = \frac{\partial W}{\partial \mathbf{F}} - p\mathbf{F}^{-T}, \qquad \mathbb{H} = \frac{\partial W}{\partial \mathbb{B}}, \tag{2.8}$$

where $p$ is the Lagrange multiplier associated with the constraint of incompressibility. One can also define an energy density function for the free-space $W_e$ [50,51]

$$W_e\left(\mathbf{F}, \mathbb{B}^*\right) = \frac{1}{2}\mu_0^{-1} J^{-1}\left[\mathbf{F}\mathbb{B}^*\right] \cdot \left[\mathbf{F}\mathbb{B}^*\right], \tag{2.9}$$

that allows us to express the pull-back of Maxwell stress in vacuum $\mathbf{P}_m$ and the referential magnetic field $\mathbb{H}^*$ as

$$\mathbf{P}_m = \frac{\partial W_e}{\partial \mathbf{F}}, \qquad \mathbb{H}^* = \frac{\partial W_e}{\partial \mathbb{B}^*}. \tag{2.10}$$

### 2.1. Variational formulation and corresponding governing equations

The functional form of the total potential energy for a magnetoelastic system, consisting of the body $\Omega_R$ and its exterior $\Omega'_R = \mathbb{R}^3 \setminus \Omega_R$ can be expressed as a function of the deformation function $\chi$, the Lagrange multiplier $p$ associated with the constraint of incompressibility, and magnetic induction in the body $\mathbb{B}$ and vacuum $\mathbb{B}^*$ [19,22],

$$E\left(\chi, p, \mathbb{B}, \mathbb{B}^*\right) = \int_{\Omega_R} W\left(\mathbf{F}, \mathbb{B}\right) dV_R - \int_{\Omega_R} p\left[J-1\right] dV_R + \int_{\Omega'_R} W^e\left(\mathbf{F}, \mathbb{B}^*\right) dV_R. \tag{2.11}$$

#### 2.1.1. Equilibrium: first variation

The partial differential equations that describe equilibrium of the magnetoelastic solid are derived as the Euler–Lagrange equations of the functional $E$ in Eq. (2.11). By considering small and random perturbations of the solution variables $\chi \to \chi + \delta\chi$, $p \to p + \delta p$, $\mathbf{F} \to \mathbf{F} + \delta\mathbf{F}$, $\mathbb{B} \to \mathbb{B} + \delta\mathbb{B}$ and $\mathbb{B}^* \to \mathbb{B}^* + \delta\mathbb{B}^*$, the total energy is written as

$$\begin{aligned} E(\chi + \delta\chi, p + \delta p, \mathbb{B} + \delta\mathbb{B}, \mathbb{B}^* + \delta\mathbb{B}^*) &= \int_{\Omega_R} W(\mathbf{F} + \delta\mathbf{F}, \mathbb{B} + \delta\mathbb{B}) dV_R - \int_{\Omega_R} [p + \delta p]\Big[[J + \delta J] - 1\Big] dV_R \\ &+ \frac{1}{2\mu_0}\int_{\Omega'_R} [J + \delta J]^{-1}\Big[[\mathbf{F} + \delta\mathbf{F}][\mathbb{B}^* + \delta\mathbb{B}^*]\Big] \cdot \Big[[\mathbf{F} + \delta\mathbf{F}][\mathbb{B}^* + \delta\mathbb{B}^*]\Big] dV_R, \end{aligned} \tag{2.12}$$

Considering only the first order increments in the above expansion, upon using (2.6), (2.8), and (2.10), and applying the Divergence theorem, we can write the first variation of the functional as [22]

$$\begin{aligned} \delta E &= \int_{\Omega_R} \Big[\left[\nabla_R \cdot \mathbf{P}\right] \cdot \delta\chi + \left[\nabla_R \times \mathbb{H}\right] \cdot \delta\mathbb{A} - [J-1]\delta p\Big] dV_R \\ &+ \int_{\partial\Omega_R} \left[\Big[\left[\mathbf{P} - \mathbf{P}_m\right] \cdot \mathbf{N}\Big] \cdot \delta\chi + \left[\mathbf{N} \times \left[\mathbb{H} - \frac{1}{\mu_0}\mathbf{C}\mathbb{B}^*\right]\right] \cdot \delta\mathbb{A}\right] dS_R \\ &+ \int_{\Omega'_R} \left[-[\nabla_R \cdot \mathbf{P}_m] \cdot \delta\chi + \frac{1}{2\mu_0}\left[\nabla \times \mathbb{H}^*\right] \cdot \delta\mathbb{A}^*\right] dV_R\,. \end{aligned} \tag{2.13}$$

Here, $\mathbf{N}$ is the outward unit normal to the boundary $\partial\Omega_R$. The governing equations of the equilibrium are obtained by setting $\delta E = 0$. Since the variations $\delta\chi, \delta\mathbb{A}, \delta\mathbb{A}^*$, and $\delta p$ are arbitrary, we arrive at the governing equations of equilibrium

$$\nabla_R \cdot \mathbf{P} = \mathbf{0} \quad \text{in } \Omega_R, \tag{2.14}$$

$$J - 1 = 0 \quad \text{in } \Omega_R, \tag{2.15}$$

$$\nabla_R \times \mathbb{H} = \mathbf{0} \quad \text{in } \Omega_R, \tag{2.16}$$

$$\nabla_R \times \mathbb{H}^* = \mathbf{0} \quad \text{in } \Omega_{R'}, \tag{2.17}$$

$$\nabla_R \cdot \mathbf{P}_m = \mathbf{0} \quad \text{in } \Omega'_R, \tag{2.18}$$

and the boundary conditions

$$[\mathbf{P} - \mathbf{P}_m] \cdot \mathbf{N} = \mathbf{0} \quad \text{on } \partial\Omega_R, \tag{2.19}$$

$$\mathbf{N} \times [\mathbb{H} - \mathbb{H}^*] = \mathbf{0} \quad \text{on } \partial\Omega_R, \tag{2.20}$$

$$[\mathbb{B} - \mathbb{B}^*] \cdot \mathbf{N} = 0 \quad \text{on } \partial\Omega_R. \tag{2.21}$$

#### 2.1.2. Critical point: second variation

To analyse the critical point of bifurcation, the perturbations in the equilibrium state must adhere to specific incremental equations and boundary conditions. They are obtained from the second variation of the total potential energy. With details provided in Appendix, the governing equations are given as

$$\nabla_R \cdot \left[W_{,\mathbf{FF}}\Delta\mathbf{F} - \left[\Delta p\left[J\mathbf{F}^{-T}\right] + p\left[J\left[\mathbf{F}^{-T} : \Delta\mathbf{F}\right]\mathbf{F}^{-T} - J\mathbf{F}^{-T}[\Delta\mathbf{F}]^T\mathbf{F}^{-T}\right]\right] + W_{,\mathbf{F}\mathbb{B}}\Delta\mathbb{B}\right] = \mathbf{0} \quad \text{in } \Omega_R \tag{2.22}$$

$$\Delta J = J\mathbf{F}^{-\mathrm{T}} \cdot \Delta\mathbf{F} = 0 \quad \text{in } \Omega_R \tag{2.23}$$

$$\nabla_R \times \left[ W_{,\mathbb{B}\mathbb{B}} \Delta\mathbb{B} + W_{,\mathbb{B}\mathbf{F}} \Delta\mathbf{F} \right] = \mathbf{0} \quad \text{in } \Omega_R \tag{2.24}$$

$$\nabla_R \times \left[ W^e_{,\mathbb{B}\mathbb{B}} \Delta\mathbb{B}^* + W^e_{,\mathbb{B}\mathbf{F}} \Delta\mathbf{F}^* \right] = \mathbf{0} \quad \text{in } \Omega'_R, \tag{2.25}$$

$$\nabla_R \cdot \left[ W^e_{,\mathbf{F}\mathbf{F}} \Delta\mathbf{F}^* + W^e_{,\mathbf{F}\mathbb{B}} \Delta\mathbb{B}^* \right] = \mathbf{0} \quad \text{in } \Omega'_R. \tag{2.26}$$

The incremental boundary conditions are given as

$$[\Delta\mathbf{P} - \Delta\mathbf{P}_m] \cdot \mathbf{N}$$
$$= \left[ W_{,\mathbf{F}\mathbf{F}} \Delta\mathbf{F} - \left[ \Delta p \left[ J\mathbf{F}^{-T} \right] + p \left[ J \left[ \mathbf{F}^{-T} \cdot \Delta\mathbf{F} \right] \mathbf{F}^{-T} - J\mathbf{F}^{-T} [\Delta\mathbf{F}]^T \mathbf{F}^{-T} \right] \right] + W_{,\mathbf{F}\mathbb{B}} \Delta\mathbb{B} - \Delta\mathbf{P}_m \right] \cdot \mathbf{N} = \mathbf{0}, \tag{2.27}$$

$$\Delta[\mathbb{H} - \mathbb{H}^*] \times \mathbf{n}_R = \left[ W_{,\mathbb{B}\mathbb{B}} \Delta\mathbb{B} + \frac{1}{2} [W_{,\mathbb{B}\mathbf{F}} + \hat{W}_{,\mathbf{F}\mathbb{B}}] \Delta\mathbf{F} - \Delta\mathbb{H}^* \right] \times \mathbf{N} = \mathbf{0}, \tag{2.28}$$

$$[\Delta\mathbb{B} - \Delta\mathbb{B}^*] \cdot \mathbf{N} = 0, \tag{2.29}$$

$$[\mathbf{U} - \mathbf{U}^*] = \mathbf{0}. \tag{2.30}$$

The expressions for $\Delta\mathbf{P}_m$ and $\Delta\mathbb{H}^*$ are given in detail in Appendix.

### 2.1.3. Specialisation to a Mooney–Rivlin type magnetoelastic energy density function

We use a prototype magnetoelastic energy density function which is a generalisation of the classical incompressible Mooney–Rivlin energy density function for numerical calculations in the later sections [5]. It is given as

$$W = \frac{1}{4}\mu \left[ [1+\gamma][I_1 - 3] + [1-\gamma][I_2 - 3] \right] + \frac{1}{2\mu_0} \left[ \alpha I_4 + \beta I_5 \right]. \tag{2.31}$$

Here $\mu, \gamma, \alpha, \beta$ are the constitutive parameters of the magnetoelastic solid under consideration.

Upon substituting the energy (2.31) into the incremental governing equations (2.22)–(2.25), we get the following equations in the component form

$$\left[ \mathcal{A}_{i\alpha j\beta} \Delta F_{j\beta} + \Pi_{i\alpha\beta} \Delta\mathbb{B}_\beta + L_{i\alpha} \Delta p \right]_{,\alpha} = 0, \tag{2.32}$$

$$L_{i\alpha} \Delta F_{i\alpha} = 0, \tag{2.33}$$

$$\varepsilon_{\nu\gamma\beta} \left[ \Pi_{i\alpha\beta} \Delta F_{i\alpha} + K_{\beta\alpha} \Delta\mathbb{B}_\alpha \right]_{,\gamma} = 0, \tag{2.34}$$

$$\varepsilon_{\nu\gamma\beta} \left[ \Pi^*_{i\alpha\beta} \Delta F^*_{i\alpha} + K^*_{\beta\alpha} \Delta\mathbb{B}^*_\alpha \right]_{,\gamma} = 0, \tag{2.35}$$

$$\left[ \mathcal{A}^*_{i\alpha j\beta} \Delta F^*_{j\beta} + \Pi^*_{i\alpha\beta} \Delta\mathbb{B}^*_\beta \right]_{,\alpha} = 0. \tag{2.36}$$

along with the boundary conditions

$$\left[ \mathcal{A}_{i\alpha j\beta} \Delta F_{j\beta} + \Pi_{i\alpha\beta} \Delta\mathbb{B}_\beta + L_{i\alpha} \Delta p - \mathcal{A}^*_{i\alpha j\beta} \Delta F^*_{j\beta} - \Pi^*_{i\alpha\beta} \Delta\mathbb{B}^*_\beta \right] N_\alpha = 0, \tag{2.37}$$

$$\varepsilon_{\nu\beta\gamma} \left[ \Pi_{i\alpha\beta} \Delta F_{i\alpha} + K_{\beta\alpha} \Delta\mathbb{B}_\alpha - \Pi^*_{i\alpha\beta} \Delta F^*_{i\alpha} - K^*_{\beta\alpha} \Delta\mathbb{B}^*_\alpha \right] N_\gamma = 0, \tag{2.38}$$

$$[\Delta\mathbb{B}_\alpha - \Delta\mathbb{B}^*_\alpha] N_\alpha = 0, \tag{2.39}$$

$$[U_\alpha - U^*_\alpha] = 0, \tag{2.40}$$

in which we have used the following definitions of the various fourth, third, and second order tensors

$$\begin{aligned}
\mathcal{A}_{i\alpha j\beta} &= \frac{\mu}{2} \left[ [1+\gamma] \left[ \delta_{ij}\delta_{\alpha\beta} \right] + [1-\gamma] \left[ F_{i\alpha}F_{j\beta} - F_{i\beta}F_{j\alpha} + C_{\gamma\gamma}\delta_{ij}\delta_{\alpha\beta} - F_{i\gamma}F_{j\gamma}\delta_{\alpha\beta} - C_{\alpha\beta}\delta_{ij} \right] \right] \\
&\quad + \mu_0^{-1}\beta \left[ \delta_{ij}\mathbb{B}_\alpha\mathbb{B}_\beta \right] - p \left[ -F^{-1}_{\beta i}F^{-1}_{\alpha j} + F^{-1}_{\beta j}F^{-1}_{\alpha i} \right], \\
\mathcal{A}^*_{i\alpha j\beta} &= \mu_0^{-1} \left[ \delta_{ij}\mathbb{B}^*_\alpha\mathbb{B}^*_\beta - \mathbb{B}^*_\alpha F_{i\gamma}\mathbb{B}^*_\gamma F^{-1}_{\beta j} - \mathbb{B}^*_\beta F_{j\gamma}\mathbb{B}^*_\gamma F^{-1}_{\alpha i} + \frac{1}{2} F_{k\gamma}\mathbb{B}^*_\gamma F_{k\nu}\mathbb{B}^*_\nu \left[ F^{-1}_{\alpha i}F^{-1}_{\beta j} + F^{-1}_{\alpha j}F^{-1}_{\beta i} \right] \right], \\
\Pi_{i\alpha\beta} &= \mu_0^{-1}\beta \left[ \delta_{\alpha\beta}F_{i\gamma}\mathbb{B}_\gamma + \mathbb{B}_\alpha F_{i\beta} \right], \\
\Pi^*_{i\alpha\beta} &= \mu_0^{-1} \left[ \delta_{\alpha\beta}F_{i\gamma}\mathbb{B}^*_\gamma + \mathbb{B}^*_\alpha F_{i\beta} - F^{-1}_{\alpha i}F_{k\beta}F_{k\gamma}\mathbb{B}^*_\gamma \right], \\
L_{i\alpha} &= -F^{-1}_{\alpha i}, \\
K_{\beta\alpha} &= \mu_0^{-1} \left[ \alpha\delta_{\alpha\beta} + \beta C_{\alpha\beta} \right], \\
K^*_{\beta\alpha} &= \mu_0^{-1} F_{k\alpha}F_{k\beta}.
\end{aligned} \tag{2.41}$$

Note that in the calculations above, the subscripts in Greek indices $(\alpha, \beta, \dots)$ correspond to differentiation with respect to the $(X_1, X_2, X_3)$ coordinate system. This is distinct from the material parameters $\alpha, \beta, \gamma$ in the energy density function (2.31).

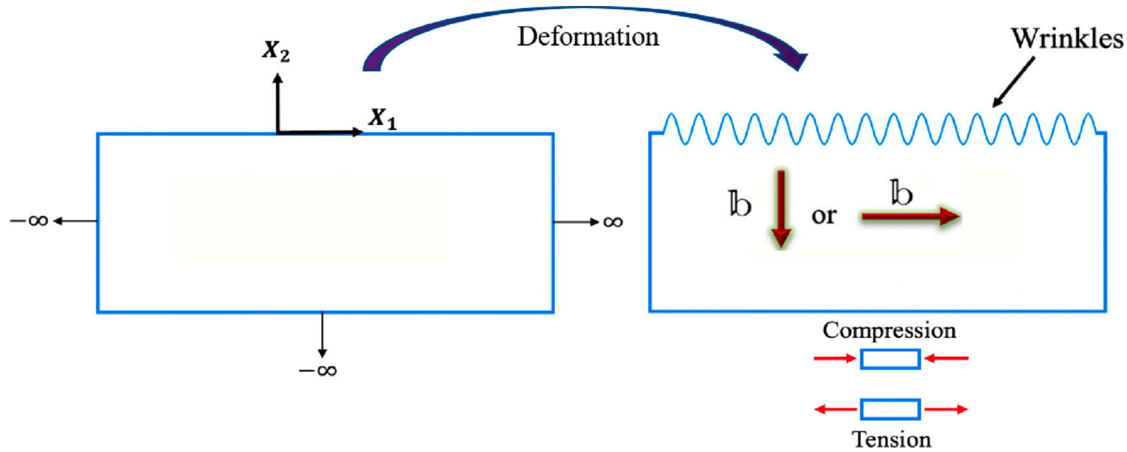


**Fig. 1.** The schematic of a magnetoelastic half-space ($X_2 < 0$) under a compression/tension mechanical load and a perpendicular/parallel magnetic field in the undeformed/deformed states.

## 3. Problem description and the corresponding equations

Consider a magnetoelastic half-space ($X_2 < 0$) with the boundary $X_2 = 0$ in its reference configuration as shown in Fig. 1. A uniform compression/tension is applied along the $X_1$ direction while maintaining the plane-strain condition in the $(X_1, X_2)$ plane. Additionally a uniform external magnetic induction is applied in either the $X_1$ or the $X_2$ direction. Consider $X_i, i = 1, 3$ be Cartesian coordinates introduced material points in the reference configuration (undeformed body) so that the coordinate $X_1$ is aligned with the direction of in-plane compression, $X_2$ is aligned perpendicular to the free surface of the undeformed half-space and $X_3$ is the out-of-plane coordinate. The deformation gradient assumes the form $[\mathbf{F}] = \mathrm{diag}(\lambda_1, \lambda_2, 1)$ where $\lambda_2 = \lambda_1^{-1}$ due to incompressibility. We aim to find the critical values of the applied stretch and magnetic induction that lead to a bifurcation of the solution in the form of surface wrinkling.

### 3.1. Uniform and incremental fields

Displacement of the points in the body are denoted by $\mathbf{u}(\mathbf{X})$. The principal plane-strain solution is denoted as $u_i^{(0)} = \left(\lambda_i - 1\right) X_i$ ($i = 1, 2$ and no sum on i). The incremental displacements $U_i, i = 1, 2$ are periodic with zero average stretch in the $X_1$ direction such that [6]

$$\mathbf{u}(X_1, X_2) = \mathbf{u}^{(0)} + \mathbf{U}(X_1, X_2). \tag{3.1}$$

The deformation gradient and its increment is given by

$$\mathbf{F} = \mathbf{I} + \frac{\partial \mathbf{u}^{(0)}}{\partial \mathbf{X}}, \quad \Delta\mathbf{F} = \frac{\partial \mathbf{U}}{\partial \mathbf{X}}, \quad \Delta\mathbf{F}^* = \frac{\partial \mathbf{U}^*}{\partial \mathbf{X}}. \tag{3.2}$$

The deformation gradient must satisfy the internal constraint of incompressibility. The incompressibility condition $J = \det[\mathbf{F} + \Delta\mathbf{F}] = 1$ gives

$$U_{1,1}U_{2,2} - U_{1,2}U_{2,1} + \lambda_2 U_{1,1} + \lambda_1 U_{2,2} = 0. \tag{3.3}$$

The uniform magnetic induction inside and outside the body are denoted by $\mathbb{b}$ and $\mathbb{b}^*$, respectively, in the current configuration. Their components are given as

$$[\mathbb{b}] = \begin{bmatrix} B_1 \\ B_2 \end{bmatrix}, \quad [\mathbb{b}^*] = \begin{bmatrix} B_1{}^* \\ B_2{}^* \end{bmatrix}, \tag{3.4}$$

The magnetic boundary conditions (2.20), (2.21) along with the use of the energy density function (2.31) require that

$$B_1^* = \left[\alpha\lambda_1^{-1} + \beta\lambda_1\right] B_1, \qquad B_2^* = B_2. \tag{3.5}$$

Their referential counterparts are given as

$$[\mathbb{B}] = \begin{bmatrix} B_1\lambda_2 \\ B_2\lambda_1 \end{bmatrix}, \qquad [\mathbb{B}^*] = \begin{bmatrix} B_1^*\lambda_2 \\ B_2\lambda_1 \end{bmatrix}. \tag{3.6}$$

Expansion of Maxwell's equation $(2.6)_2$ for incremental quantities $\Delta\mathbb{B}(\mathbf{X})$ and $\Delta\mathbb{B}^*(\mathbf{X})$ results in the following governing equations

$$\nabla_R \cdot \Delta\mathbb{B} = 0, \qquad \nabla_R \cdot \Delta\mathbb{B}^* = 0. \tag{3.7}$$

Since there is no dependence on the $X_3$ coordinate, we can write $\Delta\mathbb{B}$ and $\Delta\mathbb{B}^*$ in terms of stream functions $\varphi(\mathbf{X})$ and $\psi(\mathbf{X})$ as

$$[\Delta\mathbb{B}] = \begin{bmatrix} \varphi_{,2} \\ -\varphi_{,1} \end{bmatrix}, \qquad [\Delta\mathbb{B}^*] = \begin{bmatrix} \psi_{,2} \\ -\psi_{,1} \end{bmatrix}. \tag{3.8}$$

The Lagrange multiplier, $p$, linked to the incompressibility constraint can be determined using the boundary condition (2.19) applied to the Mooney–Rivlin model (2.31) as

$$\begin{aligned}&\Bigg[\frac{1}{4}\mu\left[[1+\gamma]\frac{\partial I_1}{\partial \mathbf{F}}+[1-\gamma]\frac{\partial I_2}{\partial \mathbf{F}}\right]+\frac{1}{2}\mu_0^{-1}\left[\alpha\frac{\partial I_4}{\partial \mathbf{F}}+\beta\frac{\partial I_5}{\partial \mathbf{F}}\right]-p\mathbf{F}^{-T}\\&-\mu_0^{-1}J^{-1}\left[\left[[\mathbf{F}\mathbb{B}^*]\otimes[\mathbf{F}\mathbb{B}^*]-\frac{1}{2}[\mathbf{F}\mathbb{B}^*]\cdot[\mathbf{F}\mathbb{B}^*]\mathbf{I}\right]\mathbf{F}^{-T}\right]\Bigg]\cdot\mathbf{N}=0,\end{aligned}\tag{3.9}$$

resulting in

$$p=\frac{1}{2}\lambda_1^{-2}\left[\mu\left[2-[\gamma-1]\lambda_1^2\right]+\mu_0^{-1}\left[\beta^2\lambda_1^4B_1^2+[2\alpha\beta\lambda_1^2B_1^2+2[\beta-\frac{1}{2}]B_2^2]\lambda_1^2+\alpha^2B_1^2\right]\right].\tag{3.10}$$

Note that based on the above expression, the Maxwell stress in vacuum can apply a non-zero traction on the half-space even if the material is purely elastic ($\alpha=\beta=0$) for the case $B_2\neq 0$.

### 3.2. Incremental governing equations

The form of the principal and incremental solutions in Section 3.1 are substituted in the governing equations (2.32)–(2.35) with the help of incremental tensors (2.41) to determine the required equations for the surface instabilities of the magnetoelastic half-space. Eq. (2.32) results in the following two equations in the body

$$\begin{aligned}&\frac{1}{2}\lambda_1^{-2}\left[\mu\left[2\lambda_1^2+1-\gamma\right]+\mu_0^{-1}\left[\beta B_1^2\right]\right]U_{1,11}+\left[\mu+\mu_0^{-1}\left[\beta\lambda_1^2B_2^2\right]\right]U_{1,22}+\frac{1}{2}\left[\mu[1-\gamma]\right]U_{2,12}-\left[\lambda_1^{-1}\right]Q_{,1}\\&+2\mu_0^{-1}\left[\beta B_1B_2\right]U_{1,12}+\mu_0^{-1}\left[\beta B_1\right]\varphi_{,12}+\mu_0^{-1}\left[\beta\lambda_1^2B_2\right]\varphi_{,22}=0,\end{aligned}\tag{3.11}$$

$$\begin{aligned}&\frac{1}{2}\mu\left[1-\gamma\right]U_{1,12}+\left[\mu+\mu_0^{-1}\left[\beta\lambda_1^{-2}B_1^2\right]\right]U_{2,11}+\left[\frac{1}{2}\mu\left[2+\lambda_1^2-\gamma\lambda_1^2\right]+\mu_0^{-1}\left[\beta B_2^2\lambda_1^2\right]\right]U_{2,22}-\left[\lambda_1\right]Q_{,2}\\&+2\mu_0^{-1}\left[\beta B_1B_2\right]U_{2,12}-\mu_0^{-1}\left[\beta B_2\right]\varphi_{,12}-\mu_0^{-1}\left[\beta\lambda_1^{-2}B_1\right]\varphi_{,11}=0.\end{aligned}\tag{3.12}$$

The incompressibility condition (2.33) provides the third equation as

$$\lambda_1^{-2}U_{1,1}+U_{2,2}=0.\tag{3.13}$$

The fourth Eq. (2.34) in the body is expanded as

$$-\left[\beta B_2\lambda_1^2\right]U_{1,22}-\left[\beta B_1\right]U_{1,12}+\left[\beta\lambda_1^{-2}B_1\right]U_{2,11}+\left[\beta B_2\right]U_{2,12}-\left[\alpha+\beta\lambda_1^{-2}\right]\varphi_{,11}-\left[\beta\lambda_1^2-\alpha\right]\varphi_{,22}=0.\tag{3.14}$$

Finally, Eq. (2.35) in vacuum is given as

$$-\left[\lambda_1^{-2}B_2\right]U^*_{1,11}-\left[\lambda_1^{-2}B_2\right]U^*_{1,22}+\left[\alpha\lambda_1^{-3}B_1+\beta\lambda_1^{-1}B_1\right]U^*_{2,11}+\left[\beta\lambda_1^3B_1+\alpha\lambda_1B_1\right]U^*_{2,22}-\left[\lambda_1^{-2}\right]\psi_{,11}-\left[\lambda_1^2\right]\psi_{,22}=0,\tag{3.15}$$

Eq. (2.36) in vacuum is given as

$$\left[\lambda_1^{-2}B_2^2\right]U^*_{1,11}+\left[\lambda_1^2B_2^2\right]U^*_{1,22}-\left[\lambda_1^{-3}B_2B_1\eta\right]U^*_{2,11}-\left[\lambda_1B_2B_1\eta\right]U^*_{2,22}+\left[\lambda_1^{-2}B_2\right]\psi_{,11}+\left[\lambda_1^2B_2\right]\psi_{,22}=0,\tag{3.16}$$

and

$$-\left[\lambda_1^{-3}B_2B_1\eta\right]U^*_{1,11}-\left[\lambda_1B_2B_1\eta\right]U^*_{1,22}+\left[\lambda_1^{-4}B_1^2\eta^2\right]U^*_{2,11}+\left[B_1^2\eta^2\right]U^*_{2,22}-\left[B_1\eta\right]\psi_{,11}-\left[B_1\lambda_1\eta\right]\psi_{,22}=0,\tag{3.17}$$

in which $\eta=\beta\lambda_1^2+\alpha$.

We define the following dimensionless quantities to non-dimensionalise the above equations

$$\bar{X}_i=\frac{X_i}{L},\quad \bar{U}_i=\frac{U_i}{L},\quad \bar{Q}=\frac{Q}{\mu},\quad \bar{\varphi}=\frac{\varphi}{\sqrt{\mu\mu_0}},\quad \bar{\psi}=\frac{\psi}{\sqrt{\mu\mu_0}},\quad T_1=\frac{B_1\lambda_2}{\sqrt{\mu_0\mu}},\quad T_2=\frac{B_2\lambda_1}{\sqrt{\mu_0\mu}}.\tag{3.18}$$

By using Eq. (3.18), multiplying (3.11)–(3.12) by $L/\mu$, and multiplying (3.14)–(3.17) are multiplied by $L\sqrt{\mu_0/\mu}$, we obtain the following non-dimensional governing equations

$$\begin{aligned}&\frac{1}{2}\lambda_1^{-2}\left[2\lambda_1^2+1-\gamma+\beta\lambda_1^2T_1^2\right]\bar{U}_{1,11}+\left[1+\beta T_2^2\right]\bar{U}_{1,22}+\frac{1}{2}\left[1-\gamma\right]\bar{U}_{2,12}-\left[\lambda_1^{-1}\right]\bar{Q}_{,1}\\&+2\left[\beta T_1T_2\right]\bar{U}_{1,12}+\left[\beta\lambda_1T_1\right]\bar{\varphi}_{,12}+\left[\beta\lambda_1T_2\right]\bar{\varphi}_{,22}=0,\end{aligned}\tag{3.19}$$

$$\begin{aligned}&\frac{1}{2}\left[1-\gamma\right]\bar{U}_{1,12}+\left[1+\beta T_1^2\right]\bar{U}_{2,11}+\left[\frac{1}{2}\left[2+\lambda_1^2-\gamma\lambda_1^2\right]+\beta T_2^2\right]\bar{U}_{2,22}-\left[\lambda_1\right]\bar{Q}_{,2}\\&+2\left[\beta T_1T_2\right]\bar{U}_{2,12}-\left[\beta\lambda_1^{-1}T_2\right]\bar{\varphi}_{,12}-\left[\beta\lambda_1^{-1}T_1\right]\bar{\varphi}_{,11}=0,\end{aligned}\tag{3.20}$$

$$\bar{U}_{2,2}+[\lambda_1^{-2}]\bar{U}_{1,1}=0,\tag{3.21}$$

$$-\left[\beta T_2\lambda_1\right]\bar{U}_{1,22}-\left[\beta\lambda_1T_1\right]\bar{U}_{1,12}+\left[\beta\lambda_1^{-1}T_1\right]\bar{U}_{2,11}+\left[\beta\lambda_1T_2\right]\bar{U}_{2,12}-\left[\alpha+\beta\lambda_1^{-2}\right]\bar{\varphi}_{,11}-\left[\beta\lambda_1^2-\alpha\right]\bar{\varphi}_{,22}=0,\tag{3.22}$$

$$-\left[\lambda_1^{-3}T_2\right]\bar{U}^*_{1,11}-\left[\lambda_1T_2\right]\bar{U}^*_{1,22}+\left[\alpha\lambda_1^{-2}T_1+\beta T_1\right]\bar{U}^*_{2,11}+\left[\beta\lambda_1^4T_1+\alpha\lambda_1^2T_1\right]\bar{U}^*_{2,22}-\left[\lambda_1^{-2}\right]\bar{\psi}_{,11}-\left[\lambda_1^2\right]\bar{\psi}_{,22}=0,\tag{3.23}$$

$$\left[\lambda_1^{-4}T_2^2\right]\bar{U}^*_{1,11}+\left[T_2^2\right]\bar{U}^*_{1,22}-\left[\lambda_1^{-3}T_2T_1\eta\right]\bar{U}^*_{2,11}-\left[\lambda_1T_2T_1\eta\right]\bar{U}^*_{2,22}+\left[\lambda_1^{-3}T_2\right]\bar{\psi}_{,11}+\left[\lambda_1T_2\right]\bar{\psi}_{,22}=0,\tag{3.24}$$

$$-\left[\lambda_1^{-3}T_2T_1\eta\right]\bar{U}^*_{1,11}-\left[\lambda_1T_2T_1\eta\right]\bar{U}^*_{1,22}+\left[\lambda_1^{-2}T_1^2\eta^2\right]\bar{U}^*_{2,11}+\left[T_1^2\lambda_1^2\eta^2\right]\bar{U}^*_{2,22}-\left[\lambda_1^{-2}T_1\eta\right]\bar{\psi}_{,11}-\left[T_1\lambda_1^2\eta\right]\bar{\psi}_{,22}=0.\tag{3.25}$$

### 3.3. Incremental boundary conditions

The form of principal and incremental solutions in Section 3.1 are substituted in the boundary conditions (2.37)–(2.39) with the help of the incremental tensors (2.41) to obtain the required boundary conditions at the top-surface of the half-space as follows.

$$\begin{aligned}&\frac{1}{2}\left[-2\mu\left[1-\gamma-\lambda_1^{-2}\right]+\mu_0^{-1}B_1^2\left[\beta^2\lambda_1^2+2\alpha\beta+\alpha^2\lambda_1^{-2}\right]+B_2^2[2\beta-1]\right]U_{2,1}+\left[\mu+\mu_0^{-1}\left[\beta\lambda_1^2B_2^2\right]\right]U_{1,2}+\mu_0^{-1}\left[\beta B_1B_2\right]U_{1,1}\\&+\mu_0^{-1}\left[\beta\lambda_1^2B_2\right]\varphi_{,2}-\mu_0^{-1}\left[\beta B_1\right]\varphi_{,1}-\mu_0^{-1}\left[\lambda_1^2B_2^2\right]U^*_{1,2}-\frac{1}{2}\mu_0^{-1}\left[B_1^2[\alpha\lambda_1^{-1}+\beta\lambda_1]^2+B_2^2\right]U^*_{2,1}\\&+\mu_0^{-1}\left[\alpha\lambda_1B_1B_2+\beta\lambda_1^3B_1B_2\right]U^*_{2,2}-\mu_0^{-1}\left[\lambda_1^2B_2\right]\psi_{,2}+\mu_0^{-1}\left[\alpha\lambda_1^{-1}B_1+\beta\lambda_1B_1\right]\psi_{,1}=0,\end{aligned}\tag{3.26}$$

$$\begin{aligned}&\frac{1}{2}\left[2\mu\left[1-\gamma+\lambda_1^{-2}\right]-\mu_0^{-1}\left[B_1^2\left[\beta^2\lambda_1^2+2\alpha\beta+\alpha^2\lambda_1^{-2}\right]+B_2^2\left[2\beta-1\right]\right]\right]U_{1,1}-\left[\lambda_1\right]Q+\mu_0^{-1}\left[\beta B_1B_2\right]U_{2,1}\\&+\frac{1}{2}\left[\mu\left[2+2\gamma+\lambda_1^2-\gamma\lambda_1^2\right]+\mu_0^{-1}\left[2\beta\lambda_1^2B_2^2\right]\right]U_{2,2}-\mu_0^{-1}\left[2\beta B_2\right]\varphi_{,1}+\mu_0^{-1}\left[\alpha\lambda_1B_1B_2+\beta\lambda_1^3B_1B_2\right]U^*_{1,2}\\&+\frac{1}{2}\mu_0^{-1}\left[B_2^2+B_1^2\left[\alpha\lambda_1^{-1}+\beta\lambda_1\right]^2\right]U^*_{1,1}-\mu_0^{-1}\left[\lambda_1^2B_1^2\left[\alpha\lambda_1^{-1}+\beta\lambda_1\right]^2\right]U^*_{2,2}+\mu_0^{-1}\left[\alpha\lambda_1B_1+\beta\lambda_1^3B_1\right]\psi_{,2}+\mu_0^{-1}\left[B_2\right]\psi_{,1}=0,\end{aligned}\tag{3.27}$$

$$\begin{aligned}&\beta\lambda_1^2B_2U_{1,2}+2\beta B_1U_{1,1}+\beta B_2U_{2,1}+\left[\beta\lambda_1^2+\alpha\right]\varphi_{,2}-B_2\lambda_1^2U^*_{1,2}-B_2U^*_{2,1}\\&\qquad-\mu_0^{-1}\left[\alpha\lambda_1^{-1}B_1+\beta\lambda_1B_1\right]U^*_{1,1}+\left[\alpha\lambda_1B_1+\beta\lambda_1^3B_1\right]U^*_{2,2}-\lambda_1^2\psi_{,2}=0,\end{aligned}\tag{3.28}$$

$$-\varphi_{,1}+\psi_{,1}=0,\tag{3.29}$$

$$U_1-U_1^*=0,\tag{3.30}$$

$$U_2-U_2^*=0.\tag{3.31}$$

Using the dimensionless variables in Eqs. (3.18) multiplying (3.26)–(3.31) by $\mu^{-1}$, $\mu^{-1}$, $\sqrt{\mu_0/\mu}$, $1/\sqrt{\mu\mu_0}$, $1/L$ and $1/L$, respectively, we get

$$\begin{aligned}&\frac{1}{2}\left[-2\left[1-\gamma-\lambda_1^{-2}\right]+T_1^2\left[\beta^2\lambda_1^4+2\alpha\beta\lambda_1^2+\alpha^2\lambda_1^2\right]+T_2^2\left[2\beta\lambda_1^{-2}-\lambda_1^{-2}\right]\right]\bar{U}_{2,1}+\left[1+\beta T_2^2\right]\bar{U}_{1,2}+\left[\beta T_1T_2\right]\bar{U}_{1,1}\\&+\left[\beta\lambda_1T_2\right]\bar{\varphi}_{,2}-\left[\beta\lambda_1T_1\right]\bar{\varphi}_{,1}-\left[T_2^2\right]\bar{U}^*_{1,2}-\frac{1}{2}\mu_0^{-1}\left[\lambda_1^2T_1^2[\alpha\lambda_1^{-1}+\beta\lambda_1]^2+\lambda_1^{-2}T_2^2\right]U^*_{2,1}+\left[\alpha\lambda_1T_1T_2+\beta\lambda_1^3T_1T_2\right]\bar{U}^*_{2,2}\\&-\left[\lambda_1T_2\right]\bar{\psi}_{,2}+\left[\alpha T_1+\beta\lambda_1^2T_1\right]\bar{\psi}_{,1}=0,\end{aligned}\tag{3.32}$$

$$\begin{aligned}&\frac{1}{2}\left[2\left[1-\gamma+\lambda_1^{-2}\right]-\left[T_1^2\left[\beta^2\lambda_1^4+2\alpha\beta\lambda_1^2+\alpha^2\right]+T_2^2\left[2\beta\lambda_1^{-2}-\lambda_1^{-2}\right]\right]\right]\bar{U}_{1,1}-\left[\lambda_1\right]\bar{Q}+\left[\beta T_1T_2\right]\bar{U}_{2,1}\\&+\frac{1}{2}\left[\left[2+2\gamma+\lambda_1^2-\gamma\lambda_1^2\right]+\left[2\beta T_2^2\right]\right]\bar{U}_{2,2}-\left[2\beta\lambda_1^{-1}T_2\right]\bar{\varphi}_{,1}+\left[\alpha\lambda_1T_1T_2+\beta\lambda_1^3T_1T_2\right]\bar{U}^*_{1,2}\\&+\frac{1}{2}\left[\lambda_1^{-2}T_2^2+T_1^2\lambda_1^2[\alpha\lambda_1^{-1}+\beta\lambda_1]^2\right]\bar{U}^*_{1,1}-\left[\lambda_1^4T_1^2[\alpha\lambda_1^{-1}+\beta\lambda_1]^2\right]\bar{U}^*_{2,2}+\left[\alpha\lambda_1^2T_1+\beta\lambda_1^4T_1\right]\bar{\psi}_{,2}+\left[\lambda_1^{-1}T_2\right]\bar{\psi}_{,1}=0,\end{aligned}\tag{3.33}$$

$$\begin{aligned}&\left[\beta\lambda_1T_2\right]\bar{U}_{1,2}+\left[2\beta\lambda_1T_1\right]\bar{U}_{1,1}+\left[\beta\lambda_1^{-1}T_2\right]\bar{U}_{2,1}+\left[\beta\lambda_1^2+\alpha\right]\bar{\varphi}_{,2}-\left[\alpha T_1+\beta\lambda_1^2T_1\right]\bar{U}^*_{1,1}-\left[T_2\lambda_1\right]\bar{U}^*_{1,2}\\&-\mu_0^{-1}[\lambda_1^{-1}T_2]U^*_{2,1}+\left[\alpha\lambda_1^2T_1+\beta\lambda_1^4T_1\right]\bar{U}^*_{2,2}-\left[\lambda_1^2\right]\bar{\psi}_{,2}=0,\end{aligned}\tag{3.34}$$

$$-\bar{\varphi}_{,1}+\bar{\psi}_{,1}=0,\tag{3.35}$$

$$\bar{U}_1-\bar{U}_1^*=0,\tag{3.36}$$

$$\bar{U}_2-\bar{U}_2^*=0.\tag{3.37}$$

## 4. Solution procedure

### 4.1. Purely mechanical half-space

To validate the model, the magnetic field is neglected and solutions obtained for surface instabilities of a purely mechanical half-space [6,25]. We consider periodic solutions for the differential equations (3.19)–(3.21)

$$\bar{U}_1=F\,e^{ks\bar{X}_2}\,\sin(k\bar{X}_1),\quad \bar{U}_2=G\,e^{ks\bar{X}_2}\,\cos(k\bar{X}_1),\quad \bar{Q}=k\lambda_1^{-1}H\,e^{ks\bar{X}_2}\,\cos(k\bar{X}_1),\tag{4.1}$$

where $F,G,H$ are constants, $k$ is the wave number, and $s$ is a scalar multiplier. Upon substituting the above ansatz in the governing equations (3.19)–(3.21), we arrive at the following matrix equation

$$[S][F,G,H]^T=0,\tag{4.2}$$

where $[S]$ is the $3\times3$ matrix of coefficients. To have a non-trivial solution for $F,G,H$ in Eq. (4.2), the determinant of $[S]$ must vanish. This condition results in a fourth order polynomial equation in $s$

$$\det(S)=\lambda_1^{-4}\left[[s-1][s+1][s\lambda_1^2-1][s\lambda_1^2+1]\right]=0.\tag{4.3}$$

The four solutions are $s_{1,3} = \pm 1$ and $s_{2,4} = \pm\lambda_1^{-2}$. Since all the solutions must decay as $\bar{X}_2 \to -\infty$, only the positive roots of $s$ are retained. By substituting $s_1$ and $s_2$ inside the matrix S, we determine the null-space of the linear system (4.2) as

$$G_1 = -F_1\left[\lambda_1^{-2}\right], \tag{4.4a}$$

$$G_2 = -F_2, \tag{4.4b}$$

$$H_1 = 0, \tag{4.4c}$$

$$H_2 = F_2\left[\lambda_1^4 - 1\right]\lambda_1^{-2}. \tag{4.4d}$$

Upon substituting the above in Eq. (4.1), we get the updated solutions as

$$\bar{U}_1 = \sum_{n=1}^{2} F_n \sin\left(k\bar{X}_1\right) \mathrm{e}^{ks_n\bar{X}_2}, \tag{4.5a}$$

$$\bar{U}_2 = \sum_{n=1}^{2} G_n \cos\left(k\bar{X}_1\right) \mathrm{e}^{ks_n\bar{X}_2}, \tag{4.5b}$$

$$\bar{Q} = k\lambda_1^{-1}\sum_{n=1}^{2} H_n \cos\left(k\bar{X}_1\right) \mathrm{e}^{ks_n\bar{X}_2}. \tag{4.5c}$$

By substituting the updated solutions (4.5) inside the boundary conditions (3.32)–(3.33) for the top surface $\bar{X}_2 = 0$, we arrive at a linear system $A_{ij}F_j = 0$, $\{i,j\} \in \{1,2\}$. The matrix A is given as

$$\begin{bmatrix} 1+\lambda_1^{-4} & 2\lambda_1^{-2} \\ -2\lambda_1^{-2} & -\lambda_1^2 - \lambda_1^{-2} \end{bmatrix}. \tag{4.6}$$

Bifurcation happens when the system allows for non-trivial solutions, that is, $\det(A_{ij}) = 0$ as

$$-\left[\left[\lambda_1 - 1\right]\left[\lambda_1 + 1\right]\left[\lambda_1^3 - \lambda_1^2 + \lambda_1 + 1\right]\left[\lambda_1^3 + \lambda_1^2 + \lambda_1 - 1\right]\right]\lambda_1^{-6} = 0, \tag{4.7}$$

The above can be solved analytically and results in the critical stretch for bifurcation as $\lambda_{cr} = 0.5437$ that is consistent with the value obtained by [6,25]. This critical stretch value is independent of the Mooney–Rivlin material parameters [31].

### *4.2. Magnetoelastic half-space*

At the boundary $\bar{X}_2 = 0$, continuity of the displacement and the deformation gradient motivates the following ansatz for the fictitious displacements $\bar{U}_1^*$ and $\bar{U}_2^*$ to be used in the boundary conditions later

$$\bar{U}_1^* = M\sin\left(k\bar{X}_1\right) e^{ks^*\bar{X}_2}, \quad \bar{U}_2^* = N\cos\left(k\bar{X}_1\right) e^{ks^*\bar{X}_2}. \tag{4.8}$$

Considering the role of magnetic induction in the magneto-elastic response of the half-space, we will focus on two distinct scenarios. First, $B_2 = 0$ with $B_1 \neq 0$ called as parallel magnetic induction, and secondly, $B_1 = 0$ with $B_2 \neq 0$ called as perpendicular magnetic induction.

#### *4.2.1. Parallel magnetic induction*

In addition to the ansatz for $\bar{U}_1, \bar{U}_2$, and $\bar{Q}$ in Eq. (4.1), and fictitious displacements of $\bar{U}_1^*$ and $\bar{U}_2^*$ in Eq. (4.8), we consider the following periodic ansatz for the magnetic variables in the body and vacuum,respectively

$$\bar{\varphi} = V\cos(k\bar{X}_1)\,e^{ks\bar{X}_2}, \tag{4.9a}$$

$$\bar{\psi} = W\cos(k\bar{X}_1)\,e^{ks^*\bar{X}_2}, \tag{4.9b}$$

where $V$ and $W$ are constants for the parallel magnetic load. Upon substituting the above ansatz in the governing equations (3.19)–(3.22) for the body, we arrive at the following matrix equation

$$[S][F,G,H,V]^T = 0. \tag{4.10}$$

where $[S]$ is the $4\times 4$ matrix of coefficients. To have a non-trivial solution for $F,G,H,V$ in Eq. (4.10), the determinant of $[S]$ must vanish. This condition results in

$$-\lambda_1^{-6}\left[[s-1][s+1][s\lambda_1^2 - 1][s\lambda_1^2 + 1]\left[\beta s^2\lambda_1^4 + \alpha[-\beta T_1^2 + s^2 - 1]\lambda_1^2 - \beta\right]\right] = 0. \tag{4.11}$$

resulting in six easily tractable solutions $s_{1,4} = \pm 1, s_{2,5} = \pm\lambda_1^{-2}$, and $s_{3,6} = \pm\lambda_1^{-1}\sqrt{\dfrac{\alpha\beta\lambda_1^2 B^2 + \alpha\lambda_1^2 + \beta}{\beta\lambda_1^2 + \alpha}}$. Since all the solutions must decay as $\bar{X}_2 \to -\infty$, only the positive roots of $s$ are retained. By substituting $s_1, s_2$ and $s_3$ inside the matrix $S$, we determine the null-space of the linear system (4.10) as

$$G_1 = -F_1\left[\lambda_1^{-2}\right], \tag{4.12a}$$

$$H_1 = 0, \tag{4.12b}$$

$$V_1 = -F_1\left[\lambda_1^{-1}T_1\right], \tag{4.12c}$$

$$G_2 = -F_2, \tag{4.12d}$$

$$H_2 = F_2\left[\beta\lambda_1^2 T_1^2 + \lambda_1^2 - \lambda_1^{-2}\right], \tag{4.12e}$$

$$V_2 = 0, \tag{4.12f}$$

$$G_3 = -F_3 \left[\beta\lambda_1^2 + \alpha\right] \lambda_1^{-1} \xi_1^{-1}, \tag{4.12g}$$

$$H_3 = 0, \tag{4.12h}$$

$$V_3 = -F_3 \left[T_1^2 \beta\lambda_1^4 + \lambda_1^4 - 1\right] \lambda_1^{-2} T_1^{-1} \xi_1^{-1}, \tag{4.12i}$$

in which

$$\xi_1 = \left[\beta\lambda_1^2 + \alpha\right] \left[T_1^2 \alpha\beta\lambda_1^2 + \alpha\lambda_1^2 + \beta\right]. \tag{4.13}$$

Substituting the ansatz (4.8) and (4.9b) in each of the governing equations (3.23)–(3.25) for the vacuum, we arrive at $s^*_{1,2} = \pm\lambda_1^{-2}$. Since the solutions in the vacuum must decay as $\bar{X}_2 \to +\infty$, only the negative root, $s^*_1 = -\lambda_1^{-2}$, is retained.

We note in passing that this null-space is necessary to conduct the post-bifurcation analysis as has been demonstrated for the purely mechanical problem [6]. The updated solutions are

$$\bar{U}_1 = \sum_{n=1}^{3} F_n \sin\left(k\bar{X}_1\right) \mathrm{e}^{k s_n \bar{X}_2}, \tag{4.14a}$$

$$\bar{U}_2 = \sum_{n=1}^{3} G_n \cos\left(k\bar{X}_1\right) \mathrm{e}^{k s_n \bar{X}_2}, \tag{4.14b}$$

$$\bar{Q} = k\lambda_1^{-1} \sum_{n=1}^{3} H_n \cos\left(k\bar{X}_1\right) \mathrm{e}^{k s_n \bar{X}_2}, \tag{4.14c}$$

$$\bar{\varphi} = \sum_{n=1}^{3} V_n \cos\left(k\bar{X}_1\right) \mathrm{e}^{k s_n \bar{X}_2}, \tag{4.14d}$$

$$\bar{\psi} = W \cos(k\bar{X}_1) e^{k s^*_1 \bar{X}_2}, \tag{4.14e}$$

$$\bar{U}^*_1 = M \sin\left(k\bar{X}_1\right) \mathrm{e}^{k s^*_1 \bar{X}_2}, \tag{4.14f}$$

$$\bar{U}^*_2 = N \cos\left(k\bar{X}_1\right) \mathrm{e}^{k s^*_1 \bar{X}_2}. \tag{4.14g}$$

By substituting the updated solutions (4.14) and (4.8) inside the boundary conditions (3.32)–(3.37) for the top surface $\bar{X}_2 = 0$, we arrive at a linear system $[A][F_1, F_2, F_3, W, M, N]^T = 0$.

The matrix $A$ is given as

$$\begin{bmatrix}
\begin{matrix} 1 + \lambda_1^{-4} \\ \frac{1}{2}T_1^2 \begin{bmatrix} \lambda_1^2\beta^2 \\ +\lambda_1^{-2}\alpha^2 \\ +2\beta\alpha \\ -2\beta \end{bmatrix} \end{matrix} & \begin{matrix} 2\lambda_1^{-2} \\ +\frac{1}{2}T_1^2 \begin{bmatrix} \lambda_1^4\beta^2 \\ +\alpha^2 \\ +2\alpha\beta\lambda_1^2 \end{bmatrix} \end{matrix} & \frac{1}{2}\begin{bmatrix} T_1^2\beta^3\lambda_1^8 + 2\alpha \\ + \left[3T_1^2\left[\alpha - \frac{2}{3}\right]\beta^2 - 2\beta\right]\lambda_1^6 \\ +\alpha\left[2 + 3T_1^2\left[\alpha + \frac{2}{3}\right]\beta\right]\lambda_1^4 \\ + \left[T_1^2\alpha^3 + 6\beta\right]\lambda_1^2 \end{bmatrix}\lambda_1^{-3}\xi_1^{-1} & -T_1\eta & 0 & \frac{1}{2}T_1^2\eta^2 \\
\begin{matrix} -2\lambda_1^{-2} \\ -\frac{1}{2}T_1^2 \begin{bmatrix} \lambda_1^4\beta^2 \\ +\lambda_1^2\alpha^2 \\ +2\alpha\beta\lambda_1^2 \end{bmatrix} \end{matrix} & \begin{matrix} -\lambda_1^2 - \lambda_1^{-2} \\ -\frac{1}{2}T_1^2 \begin{bmatrix} +2\beta\alpha\lambda_1^2 \\ +\alpha^2 \\ +\lambda_1^4\beta^2 \\ +2\beta\lambda_1^2 \end{bmatrix} \end{matrix} & \begin{matrix} -2\lambda_1^{-2} \\ -\frac{1}{2}T_1^2 \begin{bmatrix} \beta^2\lambda_1^4 + \alpha^2 \\ +2\alpha\beta\lambda_1^2 \end{bmatrix} \end{matrix} & -T_1\eta & \frac{1}{2}T_1^2\eta^2 & T_1^2\eta^2 \\
T_1\left[\beta\lambda_1 - \alpha\lambda_1^{-1}\right] & 2\beta\lambda_1 T & T_1^{-1}\begin{bmatrix} \lambda_1^{-3} - \lambda_1 \\ +\beta\lambda_1 T_1^2 \end{bmatrix} & 1 & -T_1\eta & -T_1\eta \\
-\lambda_1^{-1}T_1 & 0 & T_1^{-1}\begin{bmatrix} \lambda_1^{-2} - \lambda_1^2 \\ -\beta\lambda_1^2 T_1^2 \end{bmatrix}\xi^{-1} & -1 & 0 & 0 \\
1 & 1 & 1 & 0 & -1 & 0 \\
-\lambda_1^{-2} & -1 & -\left[\beta\lambda_1 + \lambda_1^{-1}\right]\xi_1^{-1} & 0 & 0 & -1
\end{bmatrix} \tag{4.15}$$

Bifurcation happens when the system allows for non-trivial solutions, that is, $\det(A_{ij}) = 0$.

**Neglecting $U^*_1$ and $U^*_2$:**

For the sake of completeness, we also present brief results in the case $U^*_1$ and $U^*_2$ are neglected.

Upon neglecting the terms containing $U_1^*$ and $U_2^*$ in the boundary conditions (3.32)–(3.37), the matrix $A$ for the modified linear system is given as

$$\begin{bmatrix} \begin{matrix} 1+\lambda_1^{-4} \\ +\frac{1}{2}T_1^2\begin{bmatrix}\beta^2\lambda_1^2 \\ +\alpha^2\lambda_1^{-2} \\ +2\beta\left[\alpha-1\right]\end{bmatrix}\end{matrix} & \begin{matrix} 2\lambda_1^{-2} \\ +\frac{1}{2}T_1^2\begin{bmatrix}\beta^2\lambda_1^4 \\ +2\alpha\beta\lambda_1^2 \\ +\alpha^2\end{bmatrix}\end{matrix} & \frac{1}{2}\begin{bmatrix}\left[3T_1^2\left[\alpha-\frac{2}{3}\right]\beta^2\right]\lambda_1^3 \\ +\beta^3\lambda_1^5T_1^2+2\alpha\lambda_1^{-3} \\ +\alpha\left[2+3T_1^2\left[\alpha+\frac{2}{3}\right]\beta\right]\lambda_1 \\ +\left[\alpha^3T_1^2+6\beta\right]\lambda_1^{-1}-2\beta\lambda_1^3\end{bmatrix}\xi_1^{-1} & -T_1\eta & 0 & 0 \\ \begin{matrix} -2\lambda_1^{-2} \\ -\frac{1}{2}T_1^2\begin{bmatrix}\beta^2\lambda_1^4+\alpha^2 \\ +2\alpha\beta\lambda_1^2\end{bmatrix}\end{matrix} & \begin{matrix} -\left[\lambda_1^2+\lambda_1^{-2}\right] \\ -\frac{1}{2}T_1^2\begin{bmatrix}\beta^2\lambda_1^4+\alpha^2 \\ +2\beta\left[\alpha+1\right]\lambda_1^2\end{bmatrix}\end{matrix} & \begin{matrix} -2\lambda_1^{-2} \\ -\frac{1}{2}T_1^2\begin{bmatrix}\beta^2\lambda_1^4 \\ +2\alpha\beta\lambda_1^2 \\ +\alpha^2\end{bmatrix}\end{matrix} & -T_1\eta & 0 & 0 \\ T_1\left[\beta\lambda_1-\alpha\lambda_1^{-1}\right] & 2\beta\lambda_1T_1 & \left[1+\left[\beta T_1^2-1\right]\lambda_1^4\right]\lambda_1^{-3}T_1^{-1} & 1 & 0 & 0 \\ \lambda_1^{-1}T_1 & 0 & \left[1-\left[\beta T_1^2+1\right]\lambda_1^4\right]\lambda_1^{-2}T_1^{-1}\xi_1^{-1} & -1 & 0 & 0 \\ 1 & 1 & 1 & 0 & 0 & 0 \\ -\lambda_1^{-2} & -1 & \left[-\beta\lambda_1-\lambda_1^{-1}\right]\xi_1^{-1} & 0 & 0 & 0 \end{bmatrix} \tag{4.16}$$

#### 4.2.2. Perpendicular magnetic induction

The analysis in this section follows Section 4.2.1 closely with a few minor differences. The following periodic ansatz for the magnetic variables is considered

$$\bar{\varphi} = V\sin(k\bar{X}_1)\,e^{ks\bar{X}_2}, \tag{4.17a}$$

$$\bar{\psi} = W\sin(k\bar{X}_1)\,e^{ks^*\bar{X}_2} \tag{4.17b}$$

where $V$ and $W$ are constants. Vanishing of the determinant of the $4\times 4$ matrix $S$ for the linear system $[S][F,G,H,V]^T = 0$ gives

$$-\lambda_1^{-6}\left[[s-1]\,[s+1]\left[s\lambda_1^2-1\right]\left[s\lambda_1^2+1\right]\left[\beta s^2\lambda_1^4+\left[-1+[T_2^2\beta+1]s^2\right]\alpha\lambda_1^2-\beta\right]\right]=0. \tag{4.18}$$

The six solutions are $s_{1,4}=\pm 1, s_{2,5}=\pm\lambda^{-2}$, and $s_{3,6}=\pm\lambda_1^{-1}\sqrt{\dfrac{\alpha\lambda_1^2+\beta}{\alpha\beta T_2^2+\beta\lambda_1^2+\alpha}}$. Since all the solutions must decay as $\bar{X}_2\to-\infty$, only the positive roots of $s$ are retained. By substituting $s_1, s_2$ and $s_3$ inside the matrix $S$, we determine the null-space as

$$G_1 = -F_1\left[\lambda_1^{-2}\right], \tag{4.19a}$$

$$H_1 = 0, \tag{4.19b}$$

$$V_1 = -F_1\left[\lambda_1^{-1}T_2\right], \tag{4.19c}$$

$$G_2 = -F_2, \tag{4.19d}$$

$$H_2 = -F_2\left[-\lambda_1^2+\lambda_1^{-2}+\beta\lambda_1^{-2}T_2^2\right], \tag{4.19e}$$

$$V_2 = 0, \tag{4.19f}$$

$$G_3 = -F_3\left[T_2^2\alpha\beta+\beta\lambda_1^2+\alpha\right]\lambda_1^{-1}\xi_2^{-1}, \tag{4.19g}$$

$$H_3 = 0, \tag{4.19h}$$

$$V_3 = -F_3[-\lambda_1^4+T_2^2\beta+1]\left[T_2\lambda_1\left[\alpha\lambda_1^2+\beta\right]\right]^{-1}, \tag{4.19i}$$

in which

$$\xi_2 = \sqrt{\left[\alpha\beta T_2^2+\beta\lambda_1^2+\alpha\right]\left[\alpha\lambda_1^2+\beta\right]}. \tag{4.20}$$

Substituting the ansatz (4.8) and (4.17b) in each of the governing equations (3.23)–(3.25) for the vacuum, we arrive at $s_{1,2}^* = \pm\lambda_1^{-2}$. Since the solutions in the vacuum must decay as $\bar{X}_2\to+\infty$, only the negative root, $s_1^* = -\lambda_1^{-2}$, is retained.

The updated solutions for $\bar{U}_1, \bar{U}_2, \bar{Q}, \bar{U}_1^*, \bar{U}_2^*$ follow Eqs. (4.14) and (4.8) by considering (4.19a)–(4.19i). The updated solutions for $\bar{\varphi}$ and $\bar{\psi}$ are given as

$$\bar{\varphi} = \sum_{n=1}^{3} V_n\sin\left(k\bar{X}_1\right)\,e^{ks_n\bar{X}_2}, \quad \bar{\psi} = W\sin(k\bar{X}_1)\,e^{ks_1^*\bar{X}_2}. \tag{4.21}$$

Upon substituting the above updated solutions in the boundary conditions (3.32)–(3.37) for $\bar{X}_2 = 0$, we arrive at a linear system $[A][F_1, F_2, F_3, W, M, N]^T = 0$, where the matrix $A$ is given as

$$
\begin{bmatrix}
\begin{matrix} 1+\lambda_1^{-4} \\ +\frac{1}{2}T_2^2\lambda_1^{-4}\left[2\beta-1\right] \end{matrix} &
\begin{matrix} 2\lambda_1^{-2} \\ +T_2^2\lambda_1^{-2}\left[2\beta-\frac{1}{2}\right] \end{matrix} &
\begin{bmatrix} \begin{bmatrix} \lambda_1^4+1 \\ +\left[\beta-\frac{1}{2}\right]T_2^2 \end{bmatrix} \\ \left[T_2^2\alpha\beta+\alpha+\beta\lambda_1^2\right] \end{bmatrix}\lambda_1^{-3}\xi_2^{-1} &
\lambda_1^{-1}T_2 & \lambda_1^{-2}T_2^2 & \frac{1}{2}\lambda_1^{-2}T_2^2 \\
\begin{matrix} -2\lambda_1^{-2} \\ +\frac{1}{2}T_2^2\lambda_1^{-2} \end{matrix} &
\begin{matrix} -\left[\lambda_1^2+\lambda_1^{-2}\right] \\ +T_2^2\left[-\beta\lambda_1^{-2}+\frac{1}{2}\lambda_1^{-2}\right] \end{matrix} &
\begin{bmatrix} -2\beta\lambda_1^2+\frac{1}{2}\lambda_1^{-2}T_2^2\beta \\ -2\alpha\begin{bmatrix} T_2^2\beta \\ -\frac{1}{4}T_2^2+1 \end{bmatrix} \end{bmatrix}\left[\alpha\lambda_1^2+\beta\right]^{-1} &
\lambda_1^{-1}T_2 & \frac{1}{2}\lambda_1^{-2}T_2^2 & 0 \\
T_2\begin{bmatrix} -\alpha\lambda_1^{-1} \\ +\beta\lambda_1^{-3} \end{bmatrix} &
T_2\left[2\beta\lambda_1^{-1}\right] &
\begin{bmatrix} \left[\lambda_1^4+T_2^2\beta-1\right] \\ \left[T_2^2\alpha\beta+\beta\,\lambda_1^2+\alpha\right] \end{bmatrix}\lambda_1^{-2}T_2^{-1}\xi_2^{-1} &
1 & \lambda_1^{-1}T & \lambda_1^{-1}T \\
\lambda_1^{-1}T_2 & 0 &
\begin{bmatrix} 1-\lambda_1^4 \\ +\beta T_2^2 \end{bmatrix}\left[T_2\lambda_1\left[\alpha\lambda_1^2+\beta\right]\right]^{-1} &
1 & 0 & 0 \\
1 & 1 & 1 & 0 & -1 & 0 \\
-\lambda_1^{-2} & -1 &
\begin{bmatrix} \beta\lambda_1^2+\alpha \\ +T_2\alpha\beta \end{bmatrix}\lambda_1^{-1}\xi_2^{-1} &
0 & 0 & -1
\end{bmatrix}
\tag{4.22}
$$

and bifurcation is achieved when $\det(A) = 0$.

Similar to the case considered in Section 4.2.1, if we neglect the contribution of $U_1^*$ and $U_2^*$ in the boundary conditions, then the matrix $A$ is modified as

$$
\begin{bmatrix}
\begin{matrix} 1+\lambda_1^{-4} \\ +T_2^2\begin{bmatrix} \beta\lambda_1^{-4} \\ -\frac{1}{2}\lambda_1^{-4} \end{bmatrix} \end{matrix} &
\begin{matrix} 2\lambda_1^{-2} \\ +T_2^2\begin{bmatrix} 2\beta\lambda_1^{-2} \\ -\frac{1}{2}\lambda_1^{-2} \end{bmatrix} \end{matrix} &
\left[\begin{bmatrix} \lambda_1^4+1 \\ +\left[\beta-\frac{1}{2}\right]T_2^2 \end{bmatrix}\begin{bmatrix} T_2^2\alpha\beta \\ +\alpha+\beta\lambda_1^2 \end{bmatrix}\right]\lambda_1^{-3}\xi_2^{-1} &
\lambda_1^{-1}T_2 & 0 & 0 \\
\begin{matrix} -2\lambda_1^{-2} \\ +\frac{1}{2}T_2^2\left[\lambda_1^{-2}\right] \end{matrix} &
\begin{matrix} -\left[\lambda_1^2+\lambda_1^{-2}\right] \\ +T_2^2\left[-\beta\lambda_1^{-2}+\frac{1}{2}\lambda_1^{-2}\right] \end{matrix} &
\frac{1}{2}\begin{bmatrix} T_2^2\beta\lambda_1^{-2}-4\beta\lambda_1^2 \\ -\left[4T_2^2\beta-T_2^2+4\right]\alpha \end{bmatrix}\begin{bmatrix} \alpha\lambda_1^2 \\ +\beta \end{bmatrix}^{-1} &
\lambda_1^{-1}T_2 & 0 & 0 \\
T_2\begin{bmatrix} -\alpha\lambda_1^{-1} \\ +\beta\lambda_1^{-3} \end{bmatrix} &
T_2\left[2\beta\lambda_1^{-1}\right] &
\begin{bmatrix} \left[\lambda_1^4+T_2^2\beta-1\right] \\ \left[T_2^2\alpha\beta+\beta\lambda_1^2+\alpha\right]T_2^{-1}\lambda_1^{-2} \end{bmatrix}\xi_2^{-1} &
1 & 0 & 0 \\
\lambda_1^{-1}T_2 & 0 &
\begin{bmatrix} 1-\lambda_1^4 \\ +\beta T_2^2 \end{bmatrix}\left[T_2\lambda_1\begin{bmatrix} \alpha\lambda_1^2 \\ +\beta \end{bmatrix}\right]^{-1} &
1 & 0 & 0 \\
1 & 1 & 1 & 0 & 0 & 0 \\
-\lambda_1^{-2} & -1 &
-\begin{bmatrix} \beta\lambda_1^2+\alpha \\ +T_2\alpha\beta \end{bmatrix}\lambda_1^{-1}\xi_2^{-1} &
0 & 0 & 0
\end{bmatrix}
\tag{4.23}
$$

## 5. Numerical results

Bifurcation criteria derived in Section 4 is solved numerically by implementing an iterative Newton–Raphosn and arc-length control in Mathematica using a combination of `NDSolve` and `WhenEvent` functions. Firstly, we demonstrate the difference in the solution that can arise by considering or neglecting the important fictitious displacement $\mathbf{U}^*$ in vacuum. We also show the non-physical solutions that arise as part of the numerical method that must be discounted. Then, we calculate the dependence of critical stretch on the material constants $(\alpha, \beta)$ and the magnetic load applied in parallel and perpendicular directions.

### *5.1. Choice of the correct numerical solution*

Using the equations derived in Section 4.2 for the full magnetoelastic problem, we present the dependence of the critical stretch $\lambda_{cr}$ on the parallel and perpendicular magnetic inductions with $\alpha = \beta = 0.5$ in Fig. 2. A few observations are in order. Firstly, three numerical solutions are obtained and are denoted as $\lambda^{(1)}, \lambda^{(2)}, \lambda^{(3)}$ in Fig. 2. Only $\lambda^{(1)}$ must be considered as a physical solution since other two are trivial alternatives as shown by Nowinski [4] for the purely mechanical case. Secondly, the graphs demonstrate the importance of using the arc-length continuation method to determine the solution due to the presence of a limit point in $\lambda^{(1)}$ vs $T_1$ plot. Thirdly, the physical solution has considerably different behaviour if $U_1^*$ and $U_2^*$ are considered or neglected in the boundary conditions (refer to the equations derived at the end of Sections 4.2.1 and 4.2.2). These perturbations must be included in the equations for completeness as has been demonstrated in other computational studies [52–54] but are not explicitly discussed in other more theoretical papers [5,46]. Henceforth, we present results that include the effect of $U_1^*$ and $U_2^*$ in the boundary conditions.

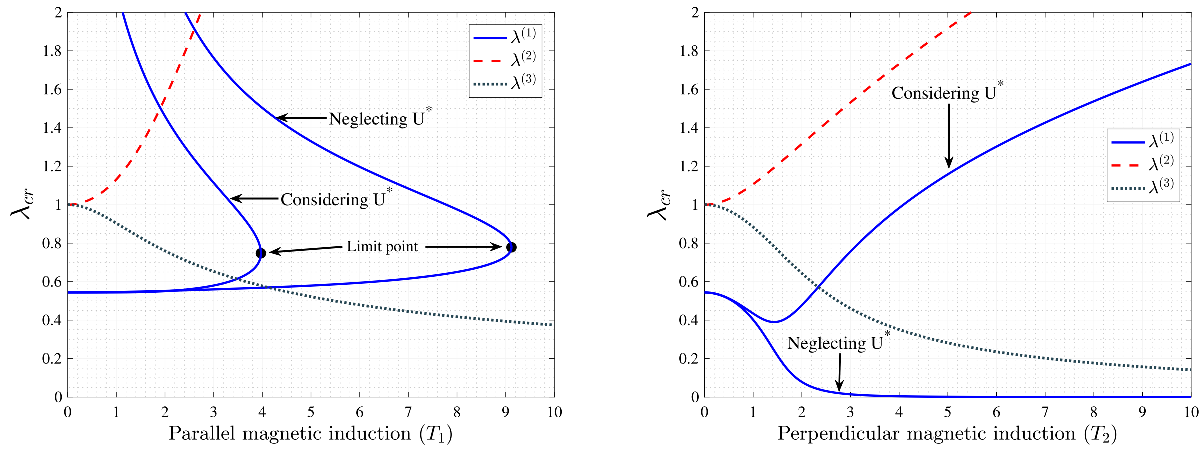


**Fig. 2.** The three numerical solutions obtained for the critical stretch $\lambda_{cr}$ as a function of the parallel magnetic induction $T_1$ and the perpendicular magnetic induction $T_2$ with $\alpha = \beta = 0.5$. Only $\lambda_1$ considering $U^*$ is the physical solution.

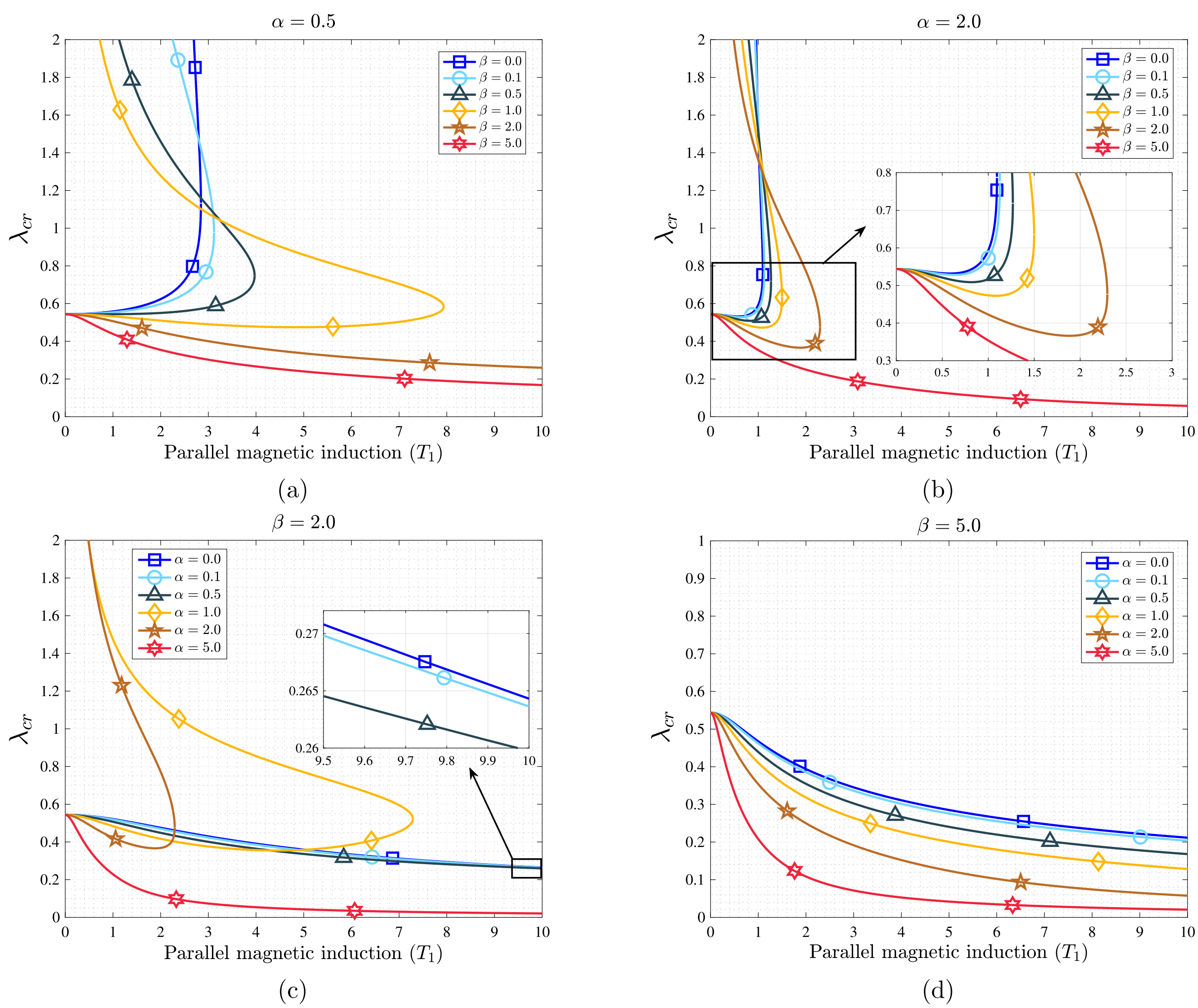


**Fig. 3.** Dependence of the critical bifurcation stretch $\lambda_{cr}$ on the applied magnetic load in the $X_1$ direction. The four graphs show the influence of the material constants $\alpha$ and $\beta$ on the bifurcation curves.

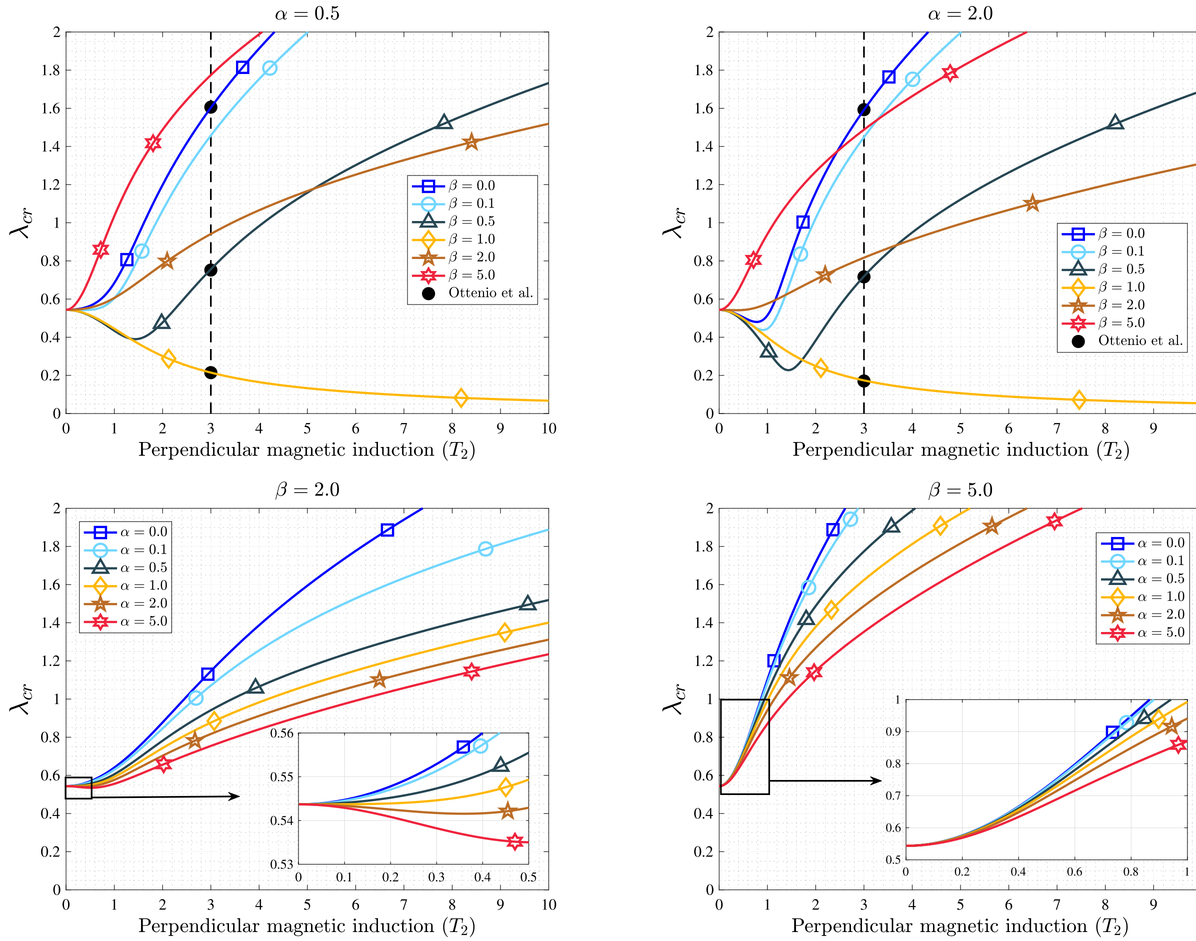


**Fig. 4.** Dependence of the critical bifurcation stretch $\lambda_{cr}$ on the applied magnetic load in the $X_2$ direction. The four graphs show the influence of the material constants $\alpha$ and $\beta$ on the bifurcation curves.

### 5.2. Parallel magnetic induction: Dependence on $T_1$

Fig. 3 shows the dependence of the critical bifurcation stretch $\lambda_{cr}$ with respect to the applied dimensionless parallel magnetic induction $T_1$. The material constant $\alpha$ is fixed and the parameter $\beta$ is varied in Figs. 3(a, b), while $\beta$ is fixed and $\alpha$ is varied in Figs. 3(c, d).

All the curves start from the critical value of the purely mechanical problem, $\lambda_{cr} = 0.54$, at zero magnetic loading. The stability curves for the parallel magnetic loading is highly nonlinear. For small to moderate values of $\alpha$ and $\beta$ as $T_1$ is increased, $\lambda_{cr}$ first decreases gradually before reaching a turning point and then snaps back and increases rapidly. It implies that no stable state is possible for the half-space with low $\beta$ values under a large $T_1$ load. A monotonic reduction in $\lambda_{cr}$ is observed only for large values of $\beta > 2$ which implies a stabilisation of the half-space upon the application of a magnetic field. The results for changing $\alpha$ with a constant $\beta$ in Fig. 3c are similar with some differences. When $\beta$ is kept constant and $\alpha \to 0$ or very large values, the critical stretch gradually but monotonically decreases with $T_1$. The snap-back after limit point behaviour is observed for moderate values of $\alpha$ indicating a nonlinear relationship of stability with the $\alpha$ parameter. For very large value of $\beta = 5$ in Fig. 3d, a monotonic reduction in $\lambda_{cr}$ is observed for all values of $\alpha$ indicating a stabilisation effect.

### 5.3. Perpendicular magnetic induction: Dependence on $T_2$

Fig. 4 shows the dependence of the critical bifurcation stretch $\lambda_{cr}$ with respect to the applied dimensionless perpendicular magnetic induction $T_2$. The material constant $\alpha$ is fixed and the parameter $\beta$ is varied in Figs. 4(a, b), while $\beta$ is fixed and $\alpha$ is varied in Figs. 4(c, d). The combined effect of magnetic load and the values of material parameters on the stability is quite nonlinear and explained below.

It is seen from Figs. 4(a, b) that for both high and low values of $\beta$ the magnetic induction $T_2$ increases the critical stretch $\lambda_{cr}$ at high $T_2$ values thereby destabilising the half-space. When $T_2$ is small, increasing the magnetic induction first stabilises and then destabilises the half-space. The only exception is the case when $\beta$ is close to 1; in this increase in $T_2$ monotonically reduces the $\lambda_{cr}$ thereby stabilising the half-space. Similar trends were reported by Otténio et al. [5], albeit for a smaller range of $T_2$. For coupling parameter values of $\beta \le 0.5$ and $\alpha \ge 0.5$, it can be seen from Fig. 4c that increasing the magnetic induction first reduces and then increases $\lambda_{cr}$. This effect is more prominent for higher values of $\alpha = 5$. For a high value of $\beta = 5$ in Fig. 4d, $\lambda_{cr}$ monotonically increases with the applied magnetic induction. An increase in the magnetic induction $T_2$ increases the critical stretch $\lambda_{cr}$, thereby destabilising the half-space with the effect being more prominent for lower $\alpha$ values. Unlike the case for parallel magnetic load discussed in Section 5.2, no limit point is observed for the perpendicular magnetic load.

## 6. Conclusion

We have developed a general mathematical formulation to analyse surface instability of a magnetoelastic half-space under both parallel and perpendicular magnetic loads. The governing equations of equilibrium and bifurcation are natural outcomes of a variational procedure. The solution process considers all the fields without any algebraic reduction and is therefore amenable to computational implementation as has been demonstrated herein. The numerical approach highlighted the significance of including fictitious displacements in the vacuum as well as a careful treatment to avoid non-physical solutions, confirming the necessity of comprehensive formulations in magnetoelastic modelling. We present new results for bifurcation phase-diagrams for parallel magnetic loads and large perpendicular magnetic loads. In parallel magnetic loads, we observed that the critical stretch decreases and then increases nonlinearly, revealing the possibility of limit points in the stability curve, a phenomenon which is absent in the perpendicular magnetic loading condition. Consequently, the numerical solution requires an arc-length approach to appropriately capture the limit points in the stability phase-space.

Overall, this work lays a foundation for further exploration of magnetoelastic materials in advanced engineering applications, particularly in fields where controlled surface morphologies are crucial, such as soft robotics, adaptive surfaces, smart sensors and biomedical devices [40–44]. The interplay between magnetic and mechanical fields in elastomers opens new avenues for designing responsive materials capable of dynamic surface modulation.

## CRediT authorship contribution statement

**Davood Shahsavari:** Data curation, Formal analysis, Investigation, Methodology, Software, Validation, Visualization, Writing – original draft, Writing – review & editing. **Prashant Saxena:** Conceptualization, Formal analysis, Funding acquisition, Methodology, Project administration, Resources, Supervision, Validation, Writing – original draft, Writing – review & editing.

## Declaration of competing interest

The authors declare that they do not have any conflict of interest.

## Acknowledgements

Davood Shahsavari's work is supported by the Engineering and Physical Sciences Research Council's Doctoral training fund. Prashant Saxena acknowledges the financial support of the Engineering and Physical Sciences Research Council via project no. EP/V030833/1.

## Appendix. Calculations for the second variation of the total energy

In order to consider the second variation of the total energy, we consider two separate perturbations of $W$ with respect to both the arguments, that is, variations $\delta\mathbf{F}, \Delta\mathbf{F}, \delta\mathbb{B}, \Delta\mathbb{B}$. An application of Taylor's series expansion gives

$$\begin{aligned} W(\mathbf{F}+\delta\mathbf{F}+\Delta\mathbf{F}, \mathbb{B}+\delta\mathbb{B}+\Delta\mathbb{B}) =& W(\mathbf{F},\mathbb{B}) + W_{,\mathbf{F}}\cdot[\delta\mathbf{F}+\Delta\mathbf{F}] + W_{,\mathbb{B}}[\delta\mathbb{B}+\Delta\mathbb{B}] \\ &+ \frac{1}{2}\Big[W_{,\mathbf{FF}}[\delta\mathbf{F}+\Delta\mathbf{F}]\Big]\cdot[\delta\mathbf{F}+\Delta\mathbf{F}] + \frac{1}{2}\Big[W_{,\mathbb{BB}}[\delta\mathbb{B}+\Delta\mathbb{B}]\Big]\cdot[\delta\mathbb{B}+\Delta\mathbb{B}] \\ &+ \frac{1}{2}[W_{,\mathbf{F}B}\Big[\delta\mathbb{B}+\Delta\mathbb{B}]\Big]\cdot[\delta\mathbf{F}+\Delta\mathbf{F}] + \frac{1}{2}\Big[W_{,\mathbb{B}\mathbf{F}}[\delta\mathbf{F}+\Delta\mathbf{F}]\Big]\cdot[\delta\mathbb{B}+\Delta\mathbb{B}], \end{aligned} \tag{A.1}$$

Similarly, we consider functions with two separate types of variations for Lagrange multiplier and energy density function in the vacuum, and by focusing exclusively on the second-order terms, the expression for the second variation is

$$\begin{aligned} \delta^2 E =& \int_{\Omega_R} \Bigg[ \Big[\frac{\partial^2 W}{\partial\mathbf{F}\partial\mathbf{F}} : \delta\mathbf{F}\Big] : \Delta\mathbf{F} - \Big[p\Big[\frac{\partial^2 (J)}{\partial\mathbf{F}\partial\mathbf{F}} : \delta\mathbf{F}\Big] : \Delta\mathbf{F} + \Delta p\delta J + \delta p \Delta J\Big] \\ &+ 2\Big[\frac{\partial^2 W}{\partial\mathbf{F}\partial B} : \delta\mathbf{F}\Big]\cdot\Delta\mathbf{F} + \Big[\frac{\partial^2 W}{\partial B\partial\mathbb{B}}\cdot\delta\mathbb{B}\Big]\cdot\Delta\mathbb{B} \Bigg] dV_R \\ &+ \int_{\Omega'_R} \Bigg[ \Big[\frac{\partial^2 W^e}{\partial\mathbf{F}\partial\mathbf{F}} : \delta\mathbf{F}\Big] : \Delta\mathbf{F} + 2\Big[\frac{\partial^2 W^e}{\partial\mathbf{F}\partial\mathbb{B}^*} : \delta\mathbf{F}\Big]\cdot\Delta\mathbf{F} + \Big[\frac{\partial^2 W}{\partial\mathbb{B}^*\partial\mathbb{B}^*}\cdot\delta\mathbb{B}^*\Big]\cdot\Delta\mathbb{B}^* \Bigg] dV_R, \end{aligned} \tag{A.2}$$

in which

$$J(\mathbf{F}+\delta\mathbf{F}+\Delta\mathbf{F}) = J + \frac{\partial J}{\partial\mathbf{F}} : (\delta\mathbf{F}+\Delta\mathbf{F}) + \frac{1}{2}\left[\frac{\partial^2 J}{\partial\mathbf{F}\partial\mathbf{F}} : (\delta\mathbf{F}+\Delta\mathbf{F})\right] : (\delta\mathbf{F}+\Delta\mathbf{F}), \delta J = J\mathbf{F}^{-T}\cdot\delta\mathbf{F}, \Delta\mathbf{F} = J\mathbf{F}^{-T}\cdot\Delta\mathbf{F}. \tag{A.3}$$

The application of the divergence theorem gives us the second variation as follows to analyse the critical point,

$$\begin{aligned} &\int_{\Omega_R} \Bigg[ -\mathrm{Div}\Big( W_{,\mathbf{FF}}\Delta\mathbf{F} - \Big[\Delta p[J\mathbf{F}^{-T}] + p[J[\mathbf{F}^{-T} : \Delta\mathbf{F}]\mathbf{F}^{-T} - J\mathbf{F}^{-T}[\Delta\mathbf{F}]^T\mathbf{F}^{-T}]\Big] + \frac{1}{2}[W_{,\mathbf{F}\mathbb{B}} + \hat{W}_{,\mathbb{B}\mathbf{F}}]\Delta\mathbb{B}\Big)\cdot\delta\chi \Bigg] dV_R \\ &+ \int_{\Omega_R} \Bigg[ -\Big[J\mathbf{F}^{-T}\Delta\mathbf{F}\Big]\cdot\delta p + \mathrm{Curl}\Big(W_{,\mathbb{BB}}\Delta\mathbb{B} + \frac{1}{2}[W_{,\mathbb{B}\mathbf{F}} + \hat{W}_{,\mathbb{B}\mathbf{F}}]\Delta\mathbf{F}\Big)\cdot\delta\mathbb{A} \Bigg] dV_R \\ &+ \int_{\Omega'_R} \Bigg[ -\mathrm{Div}(\Delta\mathbf{P}_m)\cdot\delta\chi + \mathrm{Curl}\Big(\Delta\mathbb{H}^*\Big)\cdot\delta A \Bigg] dV_R \\ &+ \int_{\partial\Omega_R} \Bigg[ \Big[ [W_{,\mathbf{FF}}\Delta\mathbf{F} + \frac{1}{2}[W_{,\mathbf{F}\mathbb{B}} + \hat{W}_{,\mathbb{B}\mathbf{F}}]\Delta\mathbb{B}] - \Big[\Delta p[J\mathbf{F}^{-T}] + p\Big[J\big[\mathbf{F}^{-T} : \Delta\mathbf{F}\big]\mathbf{F}^{-T} - J\mathbf{F}^{-T}[\Delta\mathbf{F}]^T\mathbf{F}^{-T}\Big]\Big] - \Delta\mathbf{P}_m \Big]\mathbf{N}\cdot\delta\chi \Bigg] dS_R \\ &+ \int_{\partial\Omega_R} \Bigg[ \Big[ [W_{,\mathbb{BB}}\Delta\mathbb{B} + \frac{1}{2}[W_{,\mathbb{B}\mathbf{F}}]\Delta\mathbf{F}] - \Delta\mathbb{H}^* \Big]\times\mathbf{N}\cdot\delta A + \Big[\Delta\mathbf{P}_m\mathbf{N}\cdot\delta\chi + \Delta\mathbb{H}^*\times\mathbf{N}\cdot\delta A\Big] \Bigg] dS_R = 0 \end{aligned} \tag{A.4}$$

in which $\Delta \mathbf{P}_m$ and $\Delta \mathbb{H}^*$ are

$$\Delta \mathbb{H}^* = \frac{1}{\mu_0 J}\left[-\left[\mathbf{F}^{-\mathrm{T}} \cdot \Delta \mathbf{F}^*\right]\mathbf{F}^{\mathrm{T}}\mathbf{F}\mathbb{B}^* + \left[\Delta \mathbf{F}^*\right]^{\mathrm{T}}\mathbf{F}\mathbb{B}^* + \mathbf{F}^{\mathrm{T}}\Delta \mathbf{F}^*\mathbb{B}^* + \mathbf{F}^{\mathrm{T}}\mathbf{F}\Delta \mathbb{B}^*\right], \tag{A.5}$$

and

$$\Delta \mathbf{P}_m = \frac{1}{2\mu_0 J}\left[\begin{array}{l} [\mathbf{F}\mathbb{B}^*]\cdot[\mathbf{F}\mathbb{B}^*]\Big[[\mathbf{F}^{-\mathrm{T}}\cdot\Delta \mathbf{F}^*]\mathbf{F}^{\mathrm{T}} + \mathbf{F}^{-\mathrm{T}}[\Delta \mathbf{F}^*]^{\mathrm{T}}\mathbf{F}^{-\mathrm{T}}\Big] - 2\Big[[\Delta \mathbf{F}^*\mathbb{B}^*]\cdot[\mathbf{F}\mathbb{B}^*] + [\mathbf{F}\Delta \mathbb{B}^*]\cdot[\mathbf{F}\mathbb{B}^*]\Big]\mathbf{F}^{-\mathrm{T}} \\ -2[\mathbf{F}^{-\mathrm{T}}\cdot\Delta \mathbf{F}^*][\mathbf{F}\mathbb{B}^*]\otimes\mathbb{B}^* + 2[\mathbf{F}\mathbb{B}^*]\otimes\Delta \mathbb{B}^* + 2[\mathbf{F}\Delta \mathbb{B}^*]\otimes\mathbb{B}^* + 2[\Delta \mathbf{F}^*\mathbb{B}^*]\otimes\mathbb{B}^* \end{array}\right]. \tag{A.6}$$

Within this expression, we have introduced the third-order tensors $W_{,\mathbb{B}\mathbf{F}}, \hat{W}_{,\mathbb{B}\mathbf{F}}$, which are defined based on the subsequent property:

$$[\hat{W}_{,\mathbf{F}\mathbb{B}}\mathbf{u}]\cdot\mathbf{U} = [W_{,\mathbb{B}\mathbf{F}}\mathbf{U}]\cdot\mathbf{u}. \tag{A.7}$$

## Data availability

No data was used for the research described in the article.

## References


[1] Kostas Danas, Sundeep V. Kankanala, Nicholas Triantafyllidis, Experiments and modeling of iron-particle-filled magnetorheological elastomers, J. Mech. Phys. Solids 60 (1) (2012) 120–138.
[2] Qiming Wang, Xuanhe Zhao, A three-dimensional phase diagram of growth-induced surface instabilities, Sci. Rep. 5 (1) (2015) 8887.
[3] Maurice A. Biot, Instability of a continuously inhomogeneous viscoelastic half-space under initial stress, J. Franklin Inst. 270 (3) (1960) 190–201.
[4] Jerzy L. Nowiński, Surface instability of a half-space under high two-dimensional compression, J. Franklin Inst. 288 (5) (1969).
[5] Mélanie Otténio, Michel Destrade, Raymond W. Ogden, Incremental magnetoelastic deformations, with application to surface instability, J. Elasticity 90 (2008) 19–42.
[6] Yanping Cao, John W. Hutchinson, From wrinkles to creases in elastomers: the instability and imperfection-sensitivity of wrinkling, Proc. R. Soc. A: Math. Phys. Eng. Sci. 468 (2137) (2012) 94–115.
[7] Xubo Wang, Yibin Fu, Wrinkling of a compressed hyperelastic half-space with localized surface imperfections, Int. J. Non-Linear Mech. 126 (2020) 103576.
[8] Amit Singh, Kriti Arya, Surface instability of sheared active skeletal muscle tissue with loss of muscle mass, Int. J. Non-Linear Mech. 148 (2023) 104273.
[9] Amin Saber, Ramin Sedaghati, On the modeling of magnetorheological elastomers: A state-of-the-art review, Adv. Eng. Mater. (2023).
[10] Dirk Sander, Magnetostriction and magnetoelasticity, Handb. Magn. Magn. Mater. (2020) 1–45.
[11] James P. Joule, On the effects of magnetism upon the dimensions of iron and steel bars, London, Edinb. Dublin Philos. Mag. J. Sci. 30 (199) (1847) 76–87.
[12] Mark R. Jolly, J. David Carlson, Beth C. Munoz, A model of the behaviour of magnetorheological materials, Smart Mater. Struct. 5 (5) (1996) 607.
[13] Gerlind Schubert, Philip Harrison, Large-strain behaviour of magneto-rheological elastomers tested under uniaxial compression and tension, and pure shear deformations, Polym. Test. 42 (2015) 122–134.
[14] Laurence Bodelot, Jean-Pierre Voropaieff, Tobias Pössinger, Experimental investigation of the coupled magneto-mechanical response in magnetorheological elastomers, Exp. Mech. 58 (2018) 207–221.
[15] Sergio Lucarini, Mokarram Hossain, Daniel Garcia-Gonzalez, Recent advances in hard-magnetic soft composites: Synthesis, characterisation, computational modelling, and applications, Compos. Struct. 279 (2022) 114800.
[16] N.B. Ekreem, Abdul Ghani Olabi, Tim Prescott, Aran Rafferty, Mohammed Saleem J Hashmi, An overview of magnetostriction, its use and methods to measure these properties, J. Mater. Process. Technol. 191 (1–3) (2007) 96–101.
[17] P. Saxena, M. Hossain, P. Steinmann, A theory of finite deformation magneto-viscoelasticity, Int. J. Solids Struct. 50 (24) (2013) 3886–3897.
[18] Luis Dorfmann, Raymond W. Ogden, Nonlinear magnetoelastic deformations, Q. J. Mech. Appl. Math. 57 (4) (2004) 599–622.
[19] Luis Dorfmann, Raymond W. Ogden, Nonlinear Theory of Electroelastic and Magnetoelastic Interactions, vol. 1, Springer, 2014.
[20] Clifford Truesdell, Richard Toupin, The Classical Field Theories, Springer, 1960.
[21] Roger Bustamante, Transversely isotropic nonlinear magneto-active elastomers, Acta Mech. 210 (2010) 183–214.
[22] Basant Lal Sharma, Prashant Saxena, Variational principles of nonlinear magnetoelastostatics and their correspondences, Math. Mech. Solids 26 (10) (2021) 1424–1454.
[23] Roger Bustamante, Luis Dorfmann, Raymond W. Ogden, Universal relations in isotropic nonlinear magnetoelasticity, Q. J. Mech. Appl. Math. 59 (3) (2006) 435–450.
[24] Deepak Kumar, Somnath Sarangi, Prashant Saxena, Universal relations in coupled electro-magneto-elasticity, Mech. Mater. 143 (2020) 103308.
[25] Maurice A. Biot, Surface instability of rubber in compression, Appl. Sci. Res., Sect. A 12 (2) (1963) 168–182.
[26] M. Kücken, Alan C. Newell, A model for fingerprint formation, Europhys. Lett. 68 (1) (2004) 141.
[27] Jonathan B.L. Bard, Allyson S.A. Ross, The morphogenesis of the ciliary body of the avian eye: I. Lateral cell detachment facilitates epithelial folding, Dev. Biol. 92 (1) (1982) 73–86.
[28] M Castellucci, M Schepe, I Scheffen, A Celona, P Kaufmann, The development of the human placental villous tree, Anat. Embryol. 181 (1990) 117–128.
[29] Shirley A. Bayer, Joseph Altman, The Human Brain During the Second Trimester, CRC Press, 2005.
[30] Serge Mora, Manouk Abkarian, H. Tabuteau, Y. Pomeau, Surface instability of soft solids under strain, Soft Matter 7 (22) (2011) 10612–10619.
[31] Alain Goriely, Michel Destrade, Martine Ben Amar, Instabilities in elastomers and in soft tissues, Q. J. Mech. Appl. Math. 59 (4) (2006) 615–630.
[32] Shengyou Yang, Yi-chao Chen, Wrinkle surface instability of an inhomogeneous elastic block with graded stiffness, Proc. R. Soc. A: Math. Phys. Eng. Sci. 473 (2200) (2017) 20160882.
[33] Prashant Saxena, Narravula Harshavardhan Reddy, Satya Prakash Pradhan, Magnetoelastic deformation of a circular membrane: wrinkling and limit point instabilities, Int. J. Non-Linear Mech. 116 (2019) 250–261.
[34] Attila Kossa, Megan T. Valentine, Robert M. McMeeking, Analysis of the compressible, isotropic, neo-hookean hyperelastic model, Meccanica 58 (1) (2023) 217–232.
[35] Jian Li, Nitesh Arora, Stephan Rudykh, Elastic instabilities, microstructure transformations, and pattern formations in soft materials, Curr. Opin. Solid State Mater. Sci. 25 (2) (2021) 100898.
[36] Bo Li, Yan-Ping Cao, Xi-Qiao Feng, Huajian Gao, Mechanics of morphological instabilities and surface wrinkling in soft materials: a review, Soft Matter 8 (21) (2012) 5728–5745.
[37] Lingling Chen, Xu Yang, Binglei Wang, Shengyou Yang, Nonlinear electromechanical coupling in graded soft materials: Large deformation, instability, and electroactuation, Phys. Rev. E 102 (2) (2020) 023007.
[38] Luis Dorfmann, Raymond W. Ogden, Magnetoelastic modelling of elastomers, Eur. J. Mech. A Solids 22 (4) (2003) 497–507.
[39] Roger Bustamante, MHBM Shariff, A principal axis formulation for nonlinear magnetoelastic deformations: isotropic bodies, Eur. J. Mech. A Solids 50 (2015) 17–27.
[40] Carlos Perez-Garcia, Josue Aranda-Ruiz, Maria Luisa Lopez-Donaire, Ramon Zaera, Daniel Garcia-Gonzalez, Magneto-responsive bistable structures with rate-dependent actuation modes, Adv. Funct. Mater. (2024) 2313865.
[41] Aniket Pal, Metin Sitti, Programmable mechanical devices through magnetically tunable bistable elements, Proc. Natl. Acad. Sci. 120 (15) (2023) e2212489120.
[42] Clara Gomez-Cruz, Miguel Fernandez-de la Torre, Dariusz Lachowski, Martin Prados-de Haro, Armando E del Río Hernández, Gertrudis Perea, Arrate Muñoz-Barrutia, Daniel Garcia-Gonzalez, Mechanical and functional responses in astrocytes under alternating deformation modes using magneto-active substrates, Adv. Mater. (2024) 2312497.
[43] Avinava Roy, Zenghao Zhang, Madeline K Eiken, Alan Shi, Abdon Pena-Francesch, Claudia Loebel, Programmable tissue folding patterns in structured hydrogels, Adv. Mater. (2023) 2300017.
[44] Hossein B Khaniki, Mergen H Ghayesh, Rey Chin, Marco Amabili, Hyperelastic structures: A review on the mechanics and biomechanics, Int. J. Non-Linear Mech. 148 (2023) 104275.

[45] Raymond W. Ogden, Nonlinear elasticity: incremental equations and bifurcation phenomena, in: Mathematics in Science and Engineering, vol. 185, Elsevier, 1992, pp. 437–468.
[46] Prashant Saxena, Raymond W. Ogden, On surface waves in a finitely deformed magnetoelastic half-space, Int. J. Appl. Mech. 3 (04) (2011) 633–665.
[47] Prashant Saxena, Raymond W. Ogden, On Love-type waves in a finitely deformed magnetoelastic layered half-space, Z. Angew. Math. Phys. 63 (2012) 1177–1200.
[48] Stephan Rudykh, Katia Bertoldi, Stability of anisotropic magnetorheological elastomers in finite deformations: A micromechanical approach, J. Mech. Phys. Solids 61 (4) (2013) 949–967.
[49] Luis Dorfmann, Raymond W. Ogden, Nonlinear electroelastostatics: Incremental equations and stability, Internat. J. Engrg. Sci. 48 (1) (2010) 1–14.
[50] Sundeep V. Kankanala, Nicolas Triantafyllidis, On finitely strained magnetorheological elastomers, J. Mech. Phys. Solids 52 (12) (2004) 2869–2908.
[51] Roger Bustamante, Raymond W. Ogden, Nonlinear magnetoelastostatics: Energy functionals and their second variations, Math. Mech. Solids 18 (7) (2013) 760–772.
[52] Jean-Paul Pelteret, Denis Davydov, Andrew McBride, Duc Khoi Vu, Paul Steinmann, Computational electro-elasticity and magneto-elasticity for quasi-incompressible media immersed in free space, Internat. J. Numer. Methods Engrg. 108 (11) (2016) 1307–1342.
[53] Miguel Angel Moreno-Mateos, Kostas Danas, Daniel Garcia-Gonzalez, Influence of magnetic boundary conditions on the quantitative modelling of magnetorheological elastomers, Mech. Mater. 184 (2023) 104742.
[54] Yin Liu, Shoue Chen, Xiaobo Tan, Changyong Cao, A finite element framework for magneto-actuated large deformation and instability of slender magneto-active elastomers, Int. J. Appl. Mech. 12 (01) (2020) 2050013.